

# 1



## Polarization

## Polarization

When light is incident on a linear polarizer, it will be resolved into components along and perpendicular to the polarizer direction (Figure 1.1). The parallel component – a beam polarized in the pass direction – is transmitted whereas the perpendicular component – a beam polarized perpendicular to the pass direction – will be blocked. According to Malus' Law, the amplitude of the transmitted component is

$$E_0 \cos \theta \quad (1.1)$$

where  $E_0$  is the amplitude of the incident beam and  $\theta$  is the angle between the direction of polarizer and the polarization of incident light.

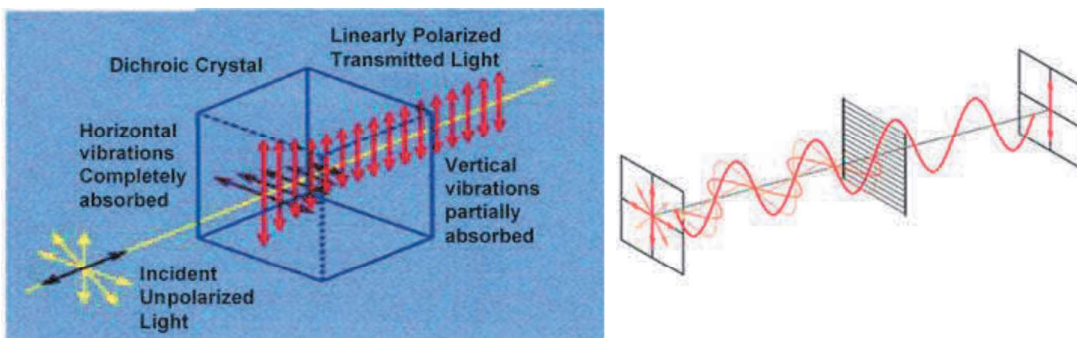


**Figure 1.1:** The concept of polarization.

When two polarizing elements are placed in succession in a beam of light, the first polarizing element is called **Polarizer** and the second element is called **Analyzer** (Figure 1.2). If the transmission axis of the analyzer (the axis of polarization) makes an angle  $\theta$  with that of the polarizer, the intensity transmitted by both polarizer and analyzer is equal to

$$I = (E_0 \cos \theta)^2 = I_0 \cos^2 \theta \quad (1.2)$$

where  $I_0$  is the intensity of the incident beam.

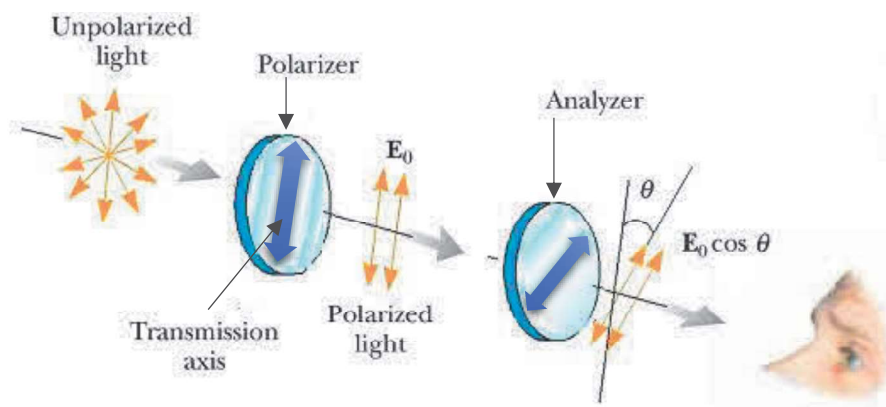
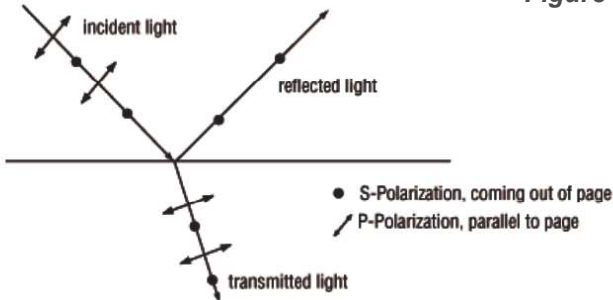


**Figure 1.2:** The concept of the Polarizer and the Analyzer.

s and p Polarization refers to the plane in which the electric field of a light wave is oscillating. s-Polarization is the plane of polarization perpendicular to the polarization axis of the polarizer (coming out of the monitor screen). p-Polarization is the plane of polarization parallel to the polarization axis of the polarizer (in the plane of the monitor screen) as shown in Figure 1.3. A linear polarizer, by design, polarizes light in the p-polarization.

**Figure 1.3:** The concept of s- and p-polarization.



### How to tell what the polarization axis is for a linear polarizer?

The axis of a linear polarizer determines the plane of polarization that the polarizer passes. There are two ways of finding the axis of a polarizer:

1. A simple method is to start with a known polarizer with a marked axis. Place both the known and unknown polarizer together and transmit light through them. Rotate the unknown polarizer until no light passes through the pair of polarizers. In this orientation, the unknown polarizer's axis is 90° from the axis of the known polarizer.
2. If a known polarizer with a marked axis cannot be found, the axis can be found by taking advantage of the Brewster effect. When light reflects at glancing incidence off of a non-metallic surface, the s-polarization is reflected more than the p-polarization. A quick way to do this is to look at the glare off of a tiled floor or another non-metallic surface. Rotate the polarizer until the glare is minimized. In this position, the polarizer is oriented so that the axis is vertical. As an example, sunglasses use polarizers that have the polarization axis vertically oriented.

Figures 1.4, 1.5 and 1.6 show varieties of the optical and in line polarizers.



**Figure 1.4:** In Line Polarizer.



Figure 1.5: Optical polarizers.

### Nanoparticle Linear Film Polarizers

- UV, VIS, NIR, and IR Spectral Ranges
- Unmounted and Mounted Versions
- Extinction Ratios up to 100 000:1
- Laser Damage Thresholds up to 25 W/cm<sup>2</sup>



Figure 1.6: Optical polarizer for Free Space.

## Circular Polarization

In circular polarization, the electric field maps out a circular pattern. That is, the two components are equal in amplitude, but 90° out of phase. When x-component is at its peak when y- component is zero, and vice-versa – the resultant traces out a circle as components oscillate.

Assume a beam  $\cos(kz - \omega t)\hat{x}$  is linearly polarized along a 45° line to the x-axis

$$\frac{E_0}{\sqrt{2}}\cos(kz - \omega t)\hat{x} + \frac{E_0}{\sqrt{2}}\cos(kz - \omega t)\hat{y} \quad (1.3)$$

where  $\hat{x}$  and  $\hat{y}$  are the unit vector along the x- and y-axis, respectively, and  $k$  is with the wave vector. By choosing the appropriate wave plate (1/4-waveplate) introduce a 90° phase shift between x- and y-components. After traversing a quarter-wave plate aligned with its crystal axes parallel to  $\hat{x}$  and  $\hat{y}$  a net phase shift of 90° will occur so that the wave can now be represented by

$$\frac{E_0}{\sqrt{2}}\cos(kz - \omega t)\hat{x} + \frac{E_0}{\sqrt{2}}\cos(kz - \omega t \mp 90^\circ)\hat{y} = \frac{E_0}{\sqrt{2}}\cos(kz - \omega t)\hat{x} - \frac{E_0}{\sqrt{2}}\sin(kz - \omega t)\hat{y}. \quad (1.4)$$

Thus, we have created circularly polarized light (Figure 1.7). The polarization rotation direction, right or left, will depend on which way the axes of the quarter-wave plate are oriented.

A wave plate is an optical element that produces some retardation between the orthogonal components of the wave. The physical origin of this retardation is due to the phenomenon of birefringence, in which the

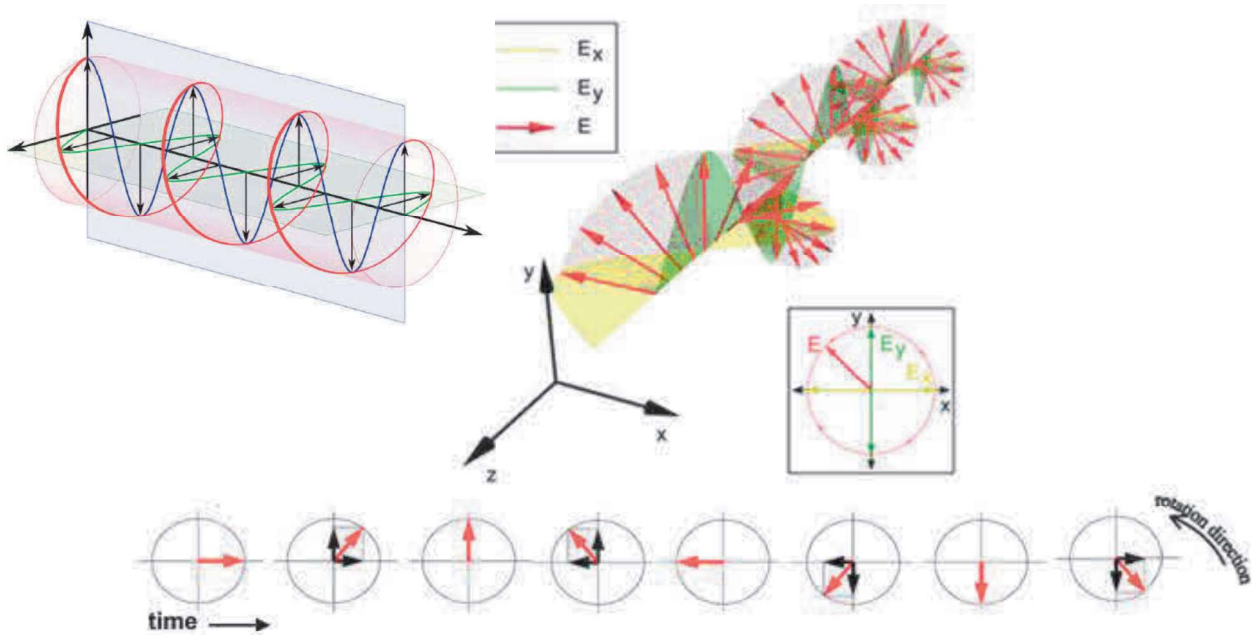


**Figure 1.7: Circular Polarization.**

components of the wave see a different refractive index (and hence have a different phase velocity) depending on the orientation of the polarization within some anisotropic material

### Superposition of two in-phase linearly polarized waves

Two linearly polarized waves in phase add to give another linearly polarized wave with a different polarization plane. Figure 1.8 presents the Superposition of two in-phase linearly polarized waves.

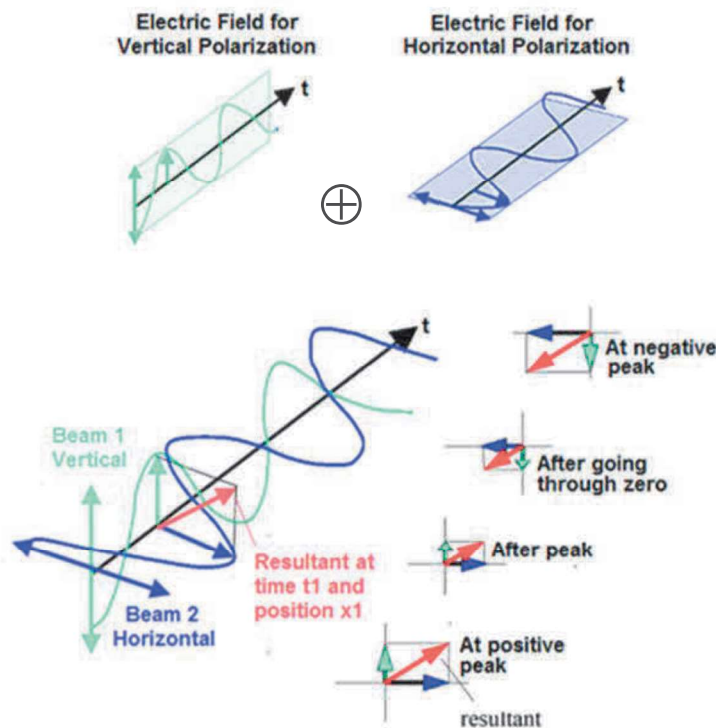


**Figure 1.8:** Superposition of two in-phase linearly polarized waves

# 2



## Light in Anisotropic Crystal

## Anisotropic Media

The electromagnetic field of a lightwave propagating through a medium exerts forces on the loosely bound outer or valence electrons. In general we would expect the field to separate the charges in a periodic manner, producing a local distribution of dipoles (Figure 2.1). Ordinarily, these forces are quite small, and in a linear isotropic medium the resulting electric polarization ( $P$ ) is parallel with and directly proportional to the applied field ( $E$ ). In effect, the polarization follows the field; if the latter is harmonic, the former will be harmonic as well. Consequently,

$$P = \epsilon_0 \chi E \quad (2.1)$$

where  $\chi$  is the dielectric susceptibility.

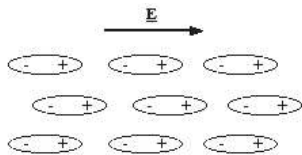


**Figure 2.1:** Separation of charges by an electric field.

As the light wave passes through the material, the oscillating electric field exerts force on movable internal charges such as alignment of polar molecules, vibrating ions in a crystal structure, or even simply electron clouds surrounding an atomic nucleus. Within the material, the actual electromagnetic disturbance depends not only on the applied field from the original wave, but also on the fields created by the displacement of these internal charges from their equilibrium positions. The effect of the displaced charges in the material (electric displacement) is

$$D = \epsilon_0 E + P = \epsilon_0 (1 + \chi) E = \epsilon E \quad (2.2)$$

and

$$n = \sqrt{\epsilon / \epsilon_0} = \sqrt{1 + \chi}. \quad (2.3)$$

Crudely speaking, as a result of having to “drag” these charges up and down with it as it goes through the material, the wave travels slower than it would be in a vacuum.

Most optical materials are linear, isotropic materials. Their internal charges respond equally to the wave’s driving electric field, regardless of its direction. Figure 2.2(a) shows a conceptual example of this, where a negative electron cloud is connected by uniform springs to a positive nucleus. Because the springs are

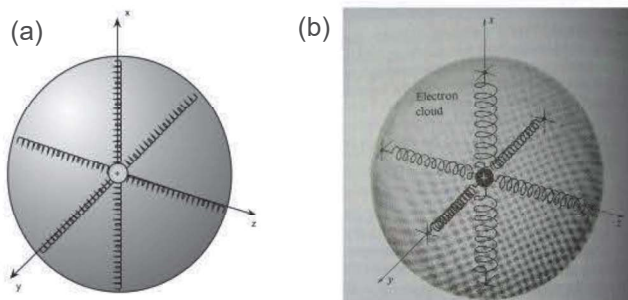


**Figure 2.2:** (a) A conceptual model of internal charge oscillators. In isotropic materials; all of the springs have the same stiffness. (b) In anisotropic media, the springs have different stiffness depending on the direction. For calcite, the springs in the horizontal direction are stiff, and the springs in the vertical (inter-plane) direction are weak.

equally strong in all directions, the displacement of the cloud due to the driving field (and therefore the polarization). That is, the internal charges do simply oscillate in line with the electric field.

The origins of anisotropy lie in any lack of symmetry in the molecules forming the material. In general, these do not have neat spherical shapes - instead, they have configurations that are characteristic of their composition, electronic structure and chemical activity. The molecular configuration in turn determines the broad classification of any crystalline solid they may form. Generally, there are seven possibilities: a crystal may be cubic, tetragonal, hexagonal, trigonal, orthorhombic, monoclinic or triclinic in structure. These systems represent the only shapes of unit cell (the basic element of a crystal lattice) that can fill all space by repetition. Figure 2.3 shows a particularly simple example, the structure of the cubic ionic crystal NaCl. Here, the  $\text{Na}^+$  and  $\text{Cl}^-$  ions are arranged in a regular lattice, which consists of three equal crystal axes, all at right angles to one another. The complete set is shown in Table 2.1 for comparison, together with some examples of common optical materials. As can be seen, the lengths of the axes may be different, and they need not be oriented at right angles. Within these systems, there are a number of subcategories, based on the possible symmetry operations that leave the lattice invariant. Each of these is called a point group, and there are a total of 32 of them. Of these, 21 are non-centrosymmetric (i.e., they lack a center of symmetry).

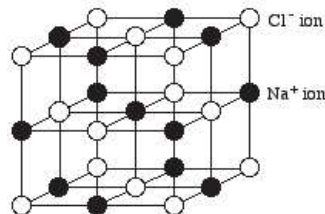


**Figure 2.3:** Cubic structure of NaCl.

Consider an isotropic crystal structure made up of widely-spaced “horizontal” planes such as for the mineral calcite, as shown in Figure 2.4. In this case, the ions in each plane are relatively free to oscillate up and down, because the bonding between planes is relatively weak; in fact, calcite easily breaks along these cleavage planes. However, the ions are locked tightly in their horizontal positions by forces from their neighboring ions. An equivalent conceptual example is shown in Figure 2.2(b), where the electron shell is now attached with stiff springs in the horizontal direction, but weak springs in the vertical direction. As a result of this asymmetry, when an electromagnetic wave enters the material, the amount of polarization depends on the direction of the applied electric field. An electric field in the vertical direction displaces the ions more than the same field would in the horizontal direction. The amount of polarization  $\mathbf{P}$  might now need a different constant of proportionality for every direction of the field. In all isotropic materials it is assumed that the result of applying a field will be independent of its direction. Furthermore, it assumes implicitly that the material polarization will also be parallel to the applied field. Although these assumptions are sometimes valid (e.g. in a truly amorphous material), in crystals (used in optoelectronics) we should generally allow for an anisotropic response in which the result of applying a field is not independent of direction; instead, the polarization depends on the field direction relative to the crystal axes:

$$\vec{\mathbf{P}} = \epsilon_0 [\chi] \vec{\mathbf{E}} \quad (2.4)$$

where the scalar fields are replaced by vector ones, to introduce some significance to field directions. Also we have exchanged the scalar dielectric susceptibility  $\chi$  for the second rank tensor term

$$[\chi] = \begin{bmatrix} \chi_{xx} & \chi_{xy} & \chi_{xz} \\ \chi_{yx} & \chi_{yy} & \chi_{yz} \\ \chi_{zx} & \chi_{zy} & \chi_{zz} \end{bmatrix} = \begin{bmatrix} \chi_x & \chi_{xy} & \chi_{xz} \\ \chi_{yx} & \chi_y & \chi_{yz} \\ \chi_{zx} & \chi_{zy} & \chi_y \end{bmatrix} \quad (2.5)$$

**Table 2.1: A summary of the lattice types**

Bravais lattice	Parameters	Simple (P)	Volume centered (I)	Base centered (C)	Face centered (F)	Crystal Axes
Triclinic  CuSO <sub>4</sub> .5H <sub>2</sub> O (copper sulphate)	$a \neq b \neq c$ $\alpha \neq \beta \neq \gamma$					A vertical axis with 2 other axes inclined to it. These are not at right angles to each other, and are of different length. 
Monoclinic  Mica MNA	$a \neq b \neq c$ $\beta = \gamma = 90^\circ$ $\alpha \neq 90^\circ$					1 vertical and 1 horizontal axis at right angles, with the other axis inclined towards the observer. All axes are of different length. 
Orthorhombic	$a \neq b \neq c$ $\alpha = \beta = \gamma = 90^\circ$					3 axes of unequal length, at right angles 
Tetragonal  BaTiO <sub>3</sub> KH <sub>2</sub> PO <sub>4</sub> (KDP) TiO <sub>2</sub> (rutile) ZrSiO <sub>4</sub> (zircon)	$a = b \neq c$ $\alpha = \beta = \gamma = 90^\circ$					3 axes at right angles; the two horizontal axes of equal length, the vertical one of different length. 
Trigonal  CaCO <sub>3</sub> (calcite) LiNbO <sub>3</sub> LiTaO <sub>3</sub> SiO <sub>2</sub> (Quartz)	$a = b = c$ $\alpha = \beta = \gamma < 120^\circ$					1 vertical and 3 horizontal axes, at angles of 120 degrees to each other. The horizontal axes of equal length. 
Cubic  Ge InP Si GaAs ZnS	$a = b = c$ $\alpha = \beta = \gamma = 90^\circ$					3 equal axes, all at right angles. 
Hexagonal	$a = b \neq c$ $\alpha = 120^\circ$ $\beta = \gamma = 90^\circ$					1 vertical and 3 horizontal axes, at angles of 120 degrees to each other. The horizontal axes of equal length. 

this allows the response of the material to be different in different directions relative to the crystal axes. In other words,

$$\begin{aligned}
 P_x &= \varepsilon_0(\chi_{xx}E_x + \chi_{xy}E_y + \chi_{xz}E_z) \\
 P_y &= \varepsilon_0(\chi_{yx}E_x + \chi_{yy}E_y + \chi_{yz}E_z) \\
 P_z &= \varepsilon_0(\chi_{zx}E_x + \chi_{zy}E_y + \chi_{zz}E_z)
 \end{aligned} \tag{2.6}$$

Considering one component of polarization (say,  $P_x$ ), it appears that there will be contributions from all three of the electric field components  $E_x$ ,  $E_y$  and  $E_z$  to  $P_x$ . Now, the relative magnitudes of the components of the susceptibility tensor depend on our choice of coordinate system, with respect to the axes of the crystal.

For a given propagation direction, the wave polarization determines the direction of the  $\mathbf{E}$  field vector. In Figure 2.4 with the widely-spaced horizontal crystal planes, an electric field in the vertical direction would find it easy to accelerate the loosely-restrained charges in this direction, and therefore zip through the

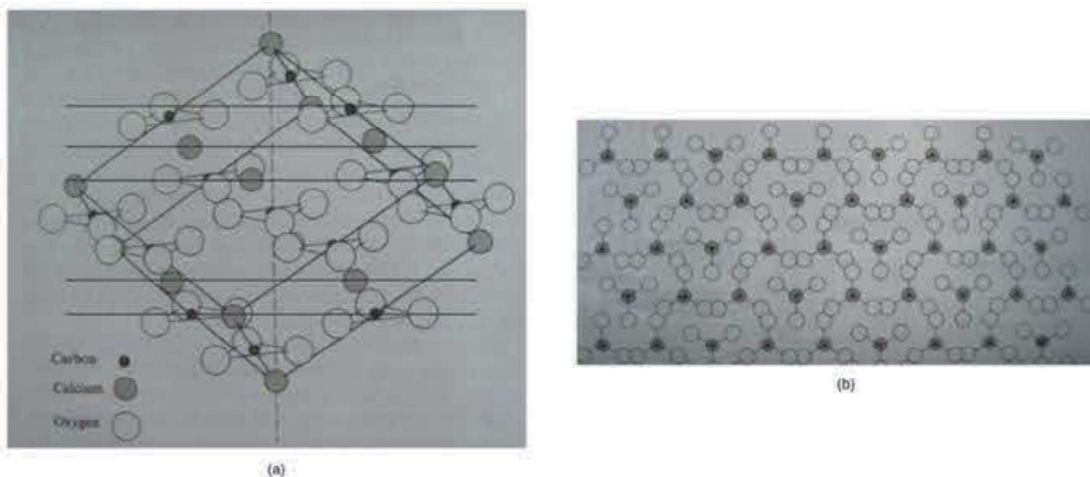


**Figure 2.4:** (a) The crystal structure of calcite. Ions lie in crystal planes (shown horizontally here), and have more freedom of motion in the vertical direction. (b) Looking down along the z-axis at the calcite structure. Rotation around z doesn't appear to cause any change in alignment or relative position of the planes.

crystal with little resistance. For a wave polarized with the field in any horizontal direction, the tightly-bound ions would resist acceleration by the applied field, the displacement would be smaller, and this wave would therefore travel slower. Light propagates through a transparent substance by exciting the atoms within the medium. The electrons are driven by the  $\mathbf{E}$  field, and they reradiate; these secondary wavelets recombine, and the resultant refracted wave moves on. The speed of the wave, and therefore the index of refraction, is determined by the difference between the frequency of the  $\mathbf{E}$  field and the natural frequency of the atoms. An anisotropy in the binding force will be manifest in an anisotropy in the refractive index. The speed of the waves is, of course, determined by the refractive index that it sees.

For the particular case in which the co-ordinate system is chosen to coincide with these principal axes, the off-axis components of the tensor are zero. We are then left with the simpler relations:

$$\begin{aligned} P_x &= \epsilon_0 \chi_x E_x \\ P_y &= \epsilon_0 \chi_y E_y \\ P_z &= \epsilon_0 \chi_z E_z. \end{aligned} \quad (2.7)$$

Even here,  $\mathbf{P}$  will only be parallel to  $\mathbf{E}$  when  $\chi_x = \chi_y = \chi_z$  and this equality holds for amorphous materials, and also for crystals with cubic symmetry. However, it does not hold for all the other crystal groups. In other words, the dielectric constant will be different for field components along each of the crystal axes

$$\vec{\mathbf{D}} = \epsilon_0(1 + [\chi])\vec{\mathbf{E}} = [\boldsymbol{\epsilon}]\vec{\mathbf{E}} \quad (2.8)$$

where

$$[\boldsymbol{\epsilon}] = \begin{bmatrix} \epsilon_{xx} & \epsilon_{xy} & \epsilon_{xz} \\ \epsilon_{yx} & \epsilon_{yy} & \epsilon_{yz} \\ \epsilon_{zx} & \epsilon_{zy} & \epsilon_{zz} \end{bmatrix} = \begin{bmatrix} \epsilon_x & \epsilon_{xy} & \epsilon_{xz} \\ \epsilon_{yx} & \epsilon_y & \epsilon_{yz} \\ \epsilon_{zx} & \epsilon_{zy} & \epsilon_z \end{bmatrix} \quad (2.9)$$

and  $\epsilon_x = \epsilon_{xx} = \epsilon_0(1 + \chi_{xx})$ ,  $\epsilon_{xy} = \epsilon_0\chi_{xy}$ , and  $\epsilon_{xz} = \epsilon_0\chi_{xz}$  and so on. Similarly, we may define a tensor  $[\boldsymbol{\epsilon}_r]$  for the relative dielectric constant, with  $n_{ij} = \sqrt{\epsilon_{ij}/\epsilon_0}$ . This allows the following classification of crystals in terms of their optical properties (Table 2.2):

- Isotropic cube (with no birefringence):

$$[\epsilon] = \begin{bmatrix} \epsilon & 0 & 0 \\ 0 & \epsilon & 0 \\ 0 & 0 & \epsilon \end{bmatrix} = \epsilon_0 \begin{bmatrix} n^2 & 0 & 0 \\ 0 & n^2 & 0 \\ 0 & 0 & n^2 \end{bmatrix} \quad (2.10)$$

- Materials in which two of the components  $\epsilon_x$ ,  $\epsilon_y$  and  $\epsilon_z$  are equal (e.g.  $\epsilon_x = \epsilon_y \neq \epsilon_z$ ) are termed uniaxial (with one optical axis). This class includes tetragonal, hexagonal and trigonal crystals:

$$[\epsilon] = \begin{bmatrix} \epsilon_x & 0 & 0 \\ 0 & \epsilon_x & 0 \\ 0 & 0 & \epsilon_z \end{bmatrix} = \epsilon_0 \begin{bmatrix} n_o^2 & 0 & 0 \\ 0 & n_o^2 & 0 \\ 0 & 0 & n_e^2 \end{bmatrix} \quad (2.11)$$

**Table 2.2: A summary of the lattice types and point groups.**

Symmetry	Crystal System	Point Group	Dielectric Tensor
Isotropic	Cubic	$\bar{4}3m$ $432$ $m\bar{3}$ $23$ $m\bar{3}m$	$\epsilon = \epsilon_0 \begin{pmatrix} n^2 & 0 & 0 \\ 0 & n^2 & 0 \\ 0 & 0 & n^2 \end{pmatrix}$
Uniaxial	Tetragonal	$\bar{4}$ $\bar{4}$ $4/m$ $422$ $4mm$ $\bar{4}2m$ $4/mmm$	
	Hexagonal	$\bar{6}$ $\bar{6}$ $6/m$ $622$ $6mm$ $\bar{6}m2$ $6/mmm$	$\epsilon = \epsilon_0 \begin{pmatrix} n_0^2 & 0 & 0 \\ 0 & n_0^2 & 0 \\ 0 & 0 & n_e^2 \end{pmatrix}$
	Trigonal	$\bar{3}$ $\bar{3}$ $32$ $3m$ $\bar{3}m$	
Biaxial	Triclinic	$\bar{1}$ $\bar{\bar{1}}$	
	Monoclinic	$2$ $m$ $2/m$	$\epsilon = \epsilon_0 \begin{pmatrix} n_1^2 & 0 & 0 \\ 0 & n_2^2 & 0 \\ 0 & 0 & n_3^2 \end{pmatrix}$
	Orthorhombic	$222$ $2mm$ $mmm$	

- Materials in which no two components are equal (e.g.  $\epsilon_x \neq \epsilon_y \neq \epsilon_z$ ) are called **biaxial** (with two optical axes). This class contains the orthorhombic, monoclinic and triclinic crystals:

$$[\epsilon] = \begin{bmatrix} \epsilon_x & 0 & 0 \\ 0 & \epsilon_y & 0 \\ 0 & 0 & \epsilon_z \end{bmatrix} = \epsilon_0 \begin{bmatrix} n_1^2 & 0 & 0 \\ 0 & n_2^2 & 0 \\ 0 & 0 & n_3^2 \end{bmatrix} \quad (2.12)$$

## Ordinary and Extraordinary Rays

### Effect of Anisotropic crystals on light propagation

A linearly-polarized plane wave with  $E$ -field aligned with one of the principal axis  $i$  propagates with phase velocity  $c/n$ . If the wave travels in the crystal with an arbitrary direction, since  $D$ ,  $E$ , and  $k$  as well as Poynting vector (energy flow)  $S = 1/2 E \times H$  are in the same plane  $\perp$  to ( $B$  and  $H$ ) and also  $D \perp (k \text{ and } H)$  as can be seen from Figure 2.5, therefore

$$D = -\frac{1}{\omega} k \times H = -\frac{n}{c} \hat{u} \times H \quad (2.13)$$

where  $k = n\omega\hat{u}/c$  and  $H \perp (k \text{ and } E)$

$$H = \frac{1}{\omega\mu_0} k \times E = -\frac{n}{\mu_0 c} \hat{u} \times E \quad (2.14)$$

Therefore,

$$D = -\frac{n^2}{\mu_0 c^2} \hat{u} \times \hat{u} \times E = n^2 \epsilon_0 [E - \hat{u}(\hat{u} \cdot E)] \quad (2.15)$$

Consider just one component of this expression and introduce the dielectric tensor,

$$D_i = n^2 \left[ \frac{D_i}{\epsilon_i} - \epsilon_0 u_i (\hat{u} \cdot E) \right] = \epsilon_0 u_i (\hat{u} \cdot E) \left( \frac{1}{\epsilon_i} - \frac{1}{n^2} \right)^{-1}. \quad (2.16)$$

Since  $D \perp \hat{u}$  then  $\hat{u} \cdot D = 0$  and

$$\sum_i u_i^2 \left( \frac{n^2}{\epsilon_i} - 1 \right)^{-1} = 1. \quad (2.17)$$

which is known as Fresnel's equation. This is quadratic in the square of the refractive index ( $n^2$ ) and therefore provides two possible solutions given a propagation direction  $\hat{u}$ . Hence the origin of the name of this phenomenon; birefringence which means literally double refraction.

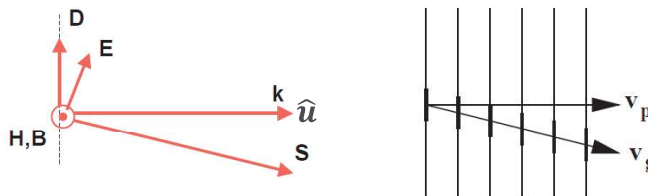


**Figure 2.5:** Optical wave characterized by  $k$ ,  $E$ ,  $D$ ,  $H$ , and  $B$  (left). Relative geometry of the field vectors and the phase ( $v_p$ ) and group velocities ( $v_g$ ) for an EM-wave in an anisotropic medium (right). The magnetic field  $H$  is directed out of the page.

Consider that case of two orthogonally polarized plane waves,  $E_e$  and  $E_o$  propagating with the same wavevector  $k$  in an anisotropic crystal. The plane perpendicular to  $k$  intersects the index ellipsoid in an ellipse. One of the axes of this ellipse is always equal to the ordinary refractive index  $n_o$ , the other is dependent on the extraordinary refractive index  $n_e$  and the angle of  $k$  to the extraordinary axis. Thus, one

of the plane waves will travel with a wave speed  $v_o = c/n_o$ , the other with wave speed  $v_e = c/n_e = c/n(\theta)$ . This leads to a phase difference between the two components as they exit the crystal. These are known as the **ordinary** and **extraordinary waves** respectively. The phenomenon of **Birefringence** occurs when the components of the wave see a different refractive index (and hence have a different phase velocity) depending on the orientation of the polarization within some anisotropic material. The ordinary ray doesn't experience any deflection. The birefringence is defined as

$$\Delta n(\theta) = n_e - n_o \quad (2.18)$$

Typical values of  $n_o$  and  $n_e$  are given in Table 2.3 for some common optical materials. Note that in some cases  $n_0$  may be greater than  $n_e$ , while the reverse is true in others.

**Table 2.3: Indices of refraction of some uniaxial crystals.**

Crystal	$n_o$	$n_e$
Calcite ( $\text{CaCO}_3$ )	1.658	1.486
Lithium niobate ( $\text{LiNbO}_3$ )	2.286	2.200
Lithium tantalate ( $\text{LiTaO}_3$ )	2.176	2.180
Quartz ( $\text{SiO}_2$ )	1.544	1.553
Rutile ( $\text{TiO}_2$ )	2.616	2.903

In general, specific directions within the crystal are special. If we look at the example shown in Figure 2.4 from above – i.e. looking down along the z axis – and rotate it around this axis, we don't observe any change in the relative alignment of the ions themselves or the crystal planes. Light propagating along this axis, regardless of its polarization, would have the **E** field in the horizontal plane. Because both polarization components would experience the same refractive index, there is no deflection or delay of either beam, and they travel together. This special direction is known as the **optical axis**. For uniaxial, optical axis is a single direction governing the optical anisotropy whereas all directions perpendicular to it (or at a given angle to it) are optically equivalent. Thus rotating the material around this axis does not change its optical behavior (Figures 2.6 and 2.7).

For a wave with the **E** field in any plane perpendicular to the optical axis, **D** and **E** are collinear and the direction of energy flow **S** (Poynting vector) and wavefront direction **k** share the usual direction as shown in Figure 2.8 (wavefront is an imaginary plane connecting all the points of constant phase). However, for any polarization direction between horizontal and vertical (for example, for a diagonally applied field  $\mathbf{E} = \sqrt{2}\hat{x} + \sqrt{2}\hat{y}$ ), the uneven spring forces in Figure 2.3(b) mean that the moveable charges get displaced significantly more in the vertical direction, but only slightly in the horizontal direction, and so the polarization **P** and displacement **D** are now in a completely different direction from **E**. This changes the direction of the energy

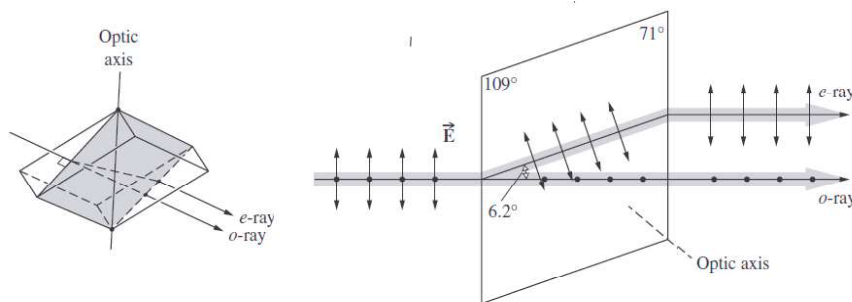


**Figure 2.6: The ordinary and extraordinary waves.**

flow ( $S = 1/2 \mathbf{E} \times \mathbf{H}$ ) away from the direction of wavefront propagation ( $k$ ). Since the physical path of the ray corresponds to the direction of the energy flow, in this situation, when light propagates in an anisotropic crystal, the ordinary beam continues in the “expected” direction while the extraordinary beam which

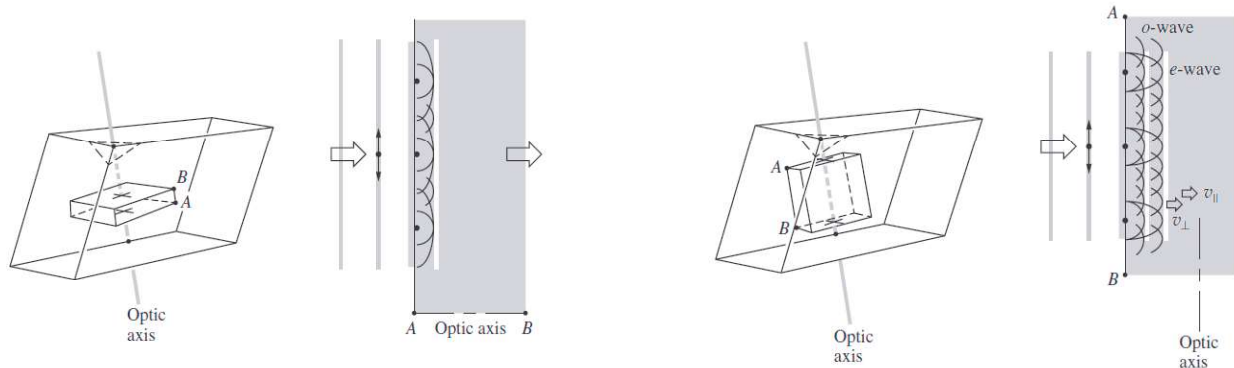


**Figure 2.7:** A calcite plate cut perpendicular to the optic axis (left). A calcite plate cut parallel to the optic axis (right).

propagates at different velocities, diverges away from the original direction of the light, shifts downward, and producing the double-image.

## Optical indicatrix (Index Ellipsoid)

It is always possible to choose a set such that the (symmetric) dielectric tensor is diagonal. The basis of this is that a symmetric matrix is specific case of a Hermitian matrix and has pure real eigenvalues and eigenvectors. Thus if we change to a new co-ordinate system where the axes are parallel to these eigenvectors, the dielectric tensor becomes diagonal

$$\frac{1}{\epsilon_0} \begin{bmatrix} D_x \\ D_y \\ D_z \end{bmatrix} = \begin{bmatrix} \epsilon_x & 0 & 0 \\ 0 & \epsilon_y & 0 \\ 0 & 0 & \epsilon_z \end{bmatrix} \begin{bmatrix} E_x \\ E_y \\ E_z \end{bmatrix}. \quad (2.19)$$

The energy density of an electric field in a birefringent dielectric is,

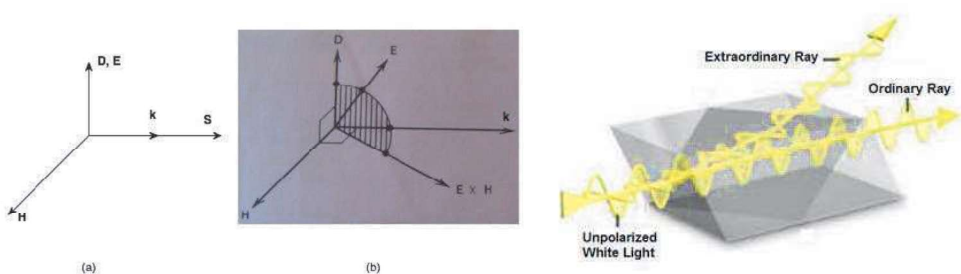


**Figure 2.8:** (a) In isotropic materials,  $\mathbf{E}$  and  $\mathbf{D}$  are always aligned, causing the direction of energy flow  $S = \mathbf{E} \times \mathbf{H}$  to coincide with the direction of wavefront propagation  $k$ . (b) Generally, in anisotropic media,  $\mathbf{E}$ ,  $\mathbf{D}$ ,  $k$  and  $S = \mathbf{E} \times \mathbf{H}$  are in different directions, but all in a plane.

$$W_E = \frac{1}{2} \vec{\mathbf{E}} \cdot \vec{\mathbf{D}} = \frac{1}{2} \left( \frac{D_x^2}{\epsilon_x} + \frac{D_y^2}{\epsilon_y} + \frac{D_z^2}{\epsilon_z} \right). \quad (2.20)$$

Substituting  $\epsilon_r = n^2$  for the various directions and setting

$$D_x/\sqrt{2W_E} = \alpha, D_y/\sqrt{2W_E} = \beta, \text{ and } D_z/\sqrt{2W_E} = \gamma \quad (2.21)$$

gives

$$\frac{\alpha^2}{n_x^2} + \frac{\beta^2}{n_y^2} + \frac{\gamma^2}{n_z^2} = 1. \quad (2.22)$$

The ellipsoid in  $(\alpha, \beta, \gamma)$  intersect the axis at  $\alpha = \pm n_x$ ,  $\beta = \pm n_y$ , and  $\gamma = \pm n_z$  (Figure 2.9a). There is a correspondence between  $(\alpha, \beta, \gamma)$  and  $(x, y, z)$ . In fact, for a wave propagating along the  $x$ -axis,  $\mathbf{D}$  vector is in  $(y, z)$  plane thus  $D_x = 0$ , therefore  $\alpha = 0$ . Similarly for a wave propagating along  $y$  (resp.  $z$ )  $\beta = 0$ , and so forth. Therefore,  $x$ -,  $y$ - and  $z$ -intercepts of the ellipsoid match the principal refractive indices  $n_x$ ,  $n_y$ ,  $n_z$ , as shown in Figure 2.9(b):

$$\frac{x^2}{n_x^2} + \frac{y^2}{n_y^2} + \frac{z^2}{n_z^2} = 1. \quad (2.23)$$

This equation represents an ellipsoid and is conventionally referred to as the index ellipsoid or optical indicatrix. The intercepts of this surface with the Cartesian axes are at  $\pm n_x$  for the  $x$ -axis, etc. This ellipsoid can be used to find the two allowed directions for the polarization and their associated refractive indices.

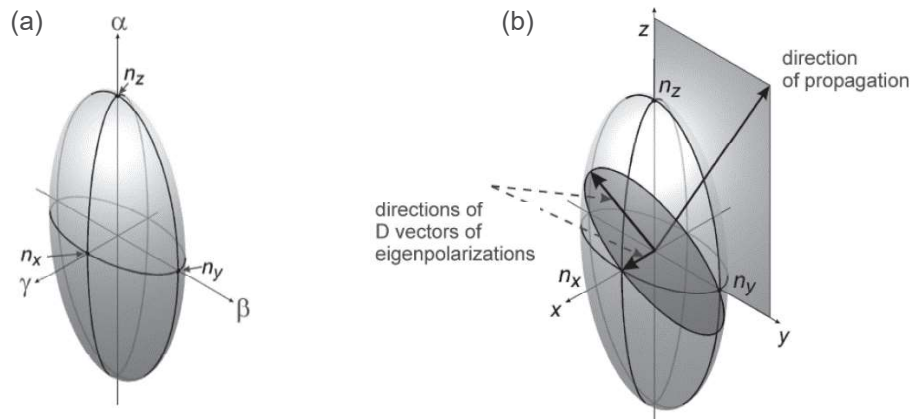


**Figure 2.9:** (a) The definition of Optical Indicatrix. (b) The correspondence between  $(\alpha, \beta, \gamma)$  and  $(x, y, z)$ .

More generally, the principle of energy conservation that the dielectric tensor must be symmetric, so that  $\epsilon_{ij} = \epsilon_{ji}$ . Similarly,

$$W_E = \frac{1}{2} \vec{\mathbf{E}} \cdot \vec{\mathbf{D}} = \frac{1}{2} \left( \frac{D_x^2}{\epsilon_x} + \frac{D_y^2}{\epsilon_y} + \frac{D_z^2}{\epsilon_z} + \frac{2D_x D_y}{\epsilon_{xy}} + \frac{2D_y D_z}{\epsilon_{yz}} + \frac{2D_z D_x}{\epsilon_{xz}} \right). \quad (2.24)$$

Note that  $2D_x D_y / \epsilon_{xy} = 2D_y D_x / \epsilon_{yx}$  and so on. Therefore,

$$\frac{x^2}{\epsilon_x} + \frac{y^2}{\epsilon_x} + \frac{z^2}{\epsilon_x} + \frac{2xy}{\epsilon_{xy}} + \frac{2yz}{\epsilon_{yz}} + \frac{2xz}{\epsilon_{xz}} = 1. \quad (2.25)$$

In an uniaxial birefringence where  $n_y = n_x$  the index ellipsoid will have cylindrical symmetry round the z-axis (optic axis). The speed of the waves depends on the refractive index that it sees which is determined by a construction known as the index ellipsoid. In the example given in Figure 2.4, both horizontal axes (x and y) had the same “spring constants”, and the z-axis was different. In these types of crystals, there is a single optical axis, and two primary refractive indices:  $n_o$  for the ordinary ray, and  $n_e$  for the extraordinary ray

$$\frac{x^2}{n_o^2} + \frac{y^2}{n_o^2} + \frac{z^2}{n_e^2} = 1 \quad (2.26)$$

where  $n_o$  and  $n_e$  are the ordinary and extraordinary refractive indices respectively (Figure 2.10).

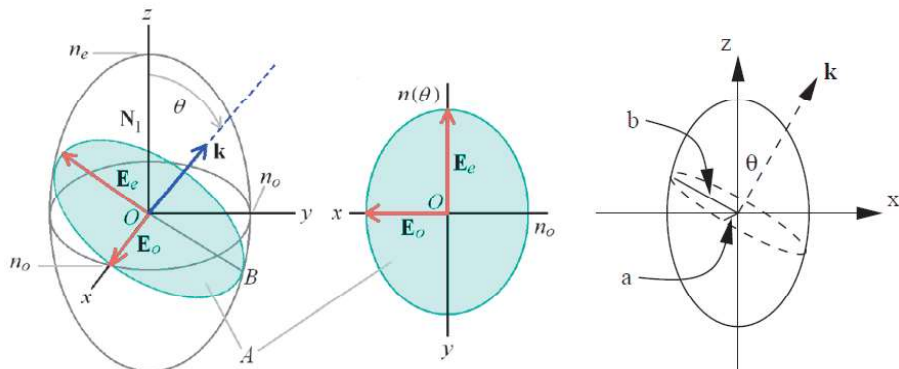


**Figure 2.10:** The index ellipsoid for a uniaxial crystal projected in 2D showing two orthogonally polarized plane waves,  $E_e$  and  $E_o$  propagating with the same wavevector  $k$ . The plane perpendicular to  $k$  intersects the index ellipsoid in an ellipse. One of the axes of this ellipse is always equal to the ordinary refractive index  $n_o$ , the other is dependent on the extraordinary refractive index  $n_e$  and the angle of  $k$  to the extraordinary axis.

The use of the index ellipsoid is as follows. Given the propagation direction of the ray  $k$  (drawn from the origin) makes an angle of  $\theta$  to the optic axis, draw a plane normal to the ray and containing the origin. The intersection of the plane with the index ellipsoid gives an ellipse. The principal axis of this ellipse give the direction of the D vector of the two linear eigenvectors. The length of the semi-minor and semi-major axis gives the index of refraction along the eigen-polarizations. In other words, the intersection of the plane normal to the direction of propagation and the index ellipsoid generates an ellipse with semi-axes  $a$  and  $b$ . For a uniaxial crystal, the semi-axis  $a$  always lies in the  $xy$ -plane and therefore has a length  $a = n_x = n_o$  independent of the angle  $\theta$ ; a ray with this polarization is the ordinary ray. The length of the other semi-axis is dependent on the angle  $\theta$ ,  $b = n_e(\theta)$ ; a ray with this polarization is the extraordinary ray. When the direction of propagation is parallel or perpendicular to the optic axis, the refractive index of the extraordinary ray can be written down immediately,

$$\begin{aligned} n_e(\theta = 0) &= n_z = n_e \\ n_e(\theta = \pi/2) &= n_x = n_o \end{aligned} \quad (2.27)$$

For the general case, we decompose  $b = n_e(\theta)$  into components parallel and perpendicular to the optic axis,  $x^2 + y^2 = n_e^2(\theta) \cos^2 \theta$  and  $z = n_e(\theta) \sin \theta$ , and insert into the equation for the index ellipsoid to give for uniaxial crystals, i.e., the wave traveling with angle  $\theta$  with respect to the ordinary axis give an index ellipse of the form

$$\frac{1}{n_e^2(\theta)} = \frac{\cos^2 \theta}{n_o^2} + \frac{\sin^2 \theta}{n_e^2}. \quad (2.28)$$

Given the dielectric tensor for a crystal, and a given light propagation direction, one very practical question is "What is the path of the ordinary and extraordinary rays through the crystal, and what are the refractive indices  $n_o$  and  $n_e(\theta)$ ?" Normal modes have refractive indices  $n_o$  and  $n_e(\theta)$  as shown in Figure 2.11:

- The minor axis corresponds to the ordinary ray. The ordinary wave has index  $n_o$  regardless of  $\theta$ . The electric field  $\mathbf{E}$  and displacement  $\mathbf{D}$  are collinear, and parallel to the minor axis.
- The major axis corresponds to the extraordinary ray. The extraordinary wave mode has refractive index  $n_e(\theta)$ . The displacement  $\mathbf{D}$  is parallel to the major axis (the electric field  $\mathbf{E}$  is orthogonal to the field of the ordinary ray, and in the plane formed by  $\mathbf{k}$  and the optical axis)  $\mathbf{E}$  and  $\mathbf{D}$  are not generally parallel.

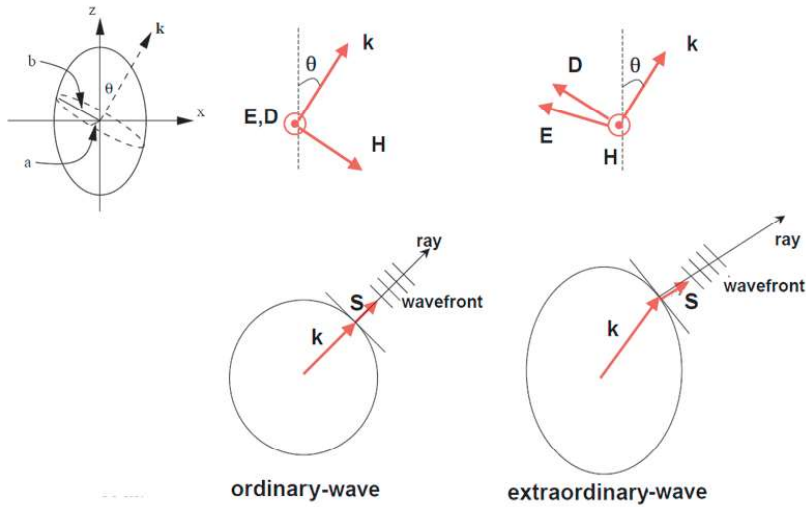


**Figure 2.11:** The path of the ordinary and extraordinary rays through the crystal.

From Maxwell's equations

$$\mathbf{k} \times (\mathbf{k} \times \mathbf{E}) - \mu_0 \epsilon \omega^2 \mathbf{E} = M \mathbf{E} = 0 \quad (2.29)$$

where

$$M = \begin{bmatrix} n_1^2 k_0^2 - k_2^2 - k_3^2 & k_2 k_1 & k_3 k_1 \\ k_1 k_2 & n_2^2 k_0^2 - k_1^2 - k_3^2 & k_3 k_2 \\ k_1 k_3 & k_2 k_3 & n_3^2 k_0^2 - k_1^2 - k_2^2 \end{bmatrix}. \quad (2.30)$$

Since the non-trivial solution is determinant of  $M$  vanishes, or  $|M|=0$  which provides the dispersion relation  $\omega = \omega(\mathbf{k})$ . The group velocity is  $v_g = \nabla_k \omega(\mathbf{k})$  and the Poynting vector  $\mathbf{S}$  is parallel to the group velocity. The equation for the  $\mathbf{k}$  surface becomes (Figure 2.12):

$$(k^2 - n_0 k_0^2) \left( \frac{k_1^2 + k_2^2}{n_e^2} + \frac{k_3^2}{n_o^2} - k_0^2 \right) = 0. \quad (2.31)$$

A second surface, a plane normal to the wavefront direction  $\mathbf{k}$  and passing through the origin,

$$x k_x + y k_y + z k_z = 0 \quad (2.32)$$

intersects the ellipsoid.

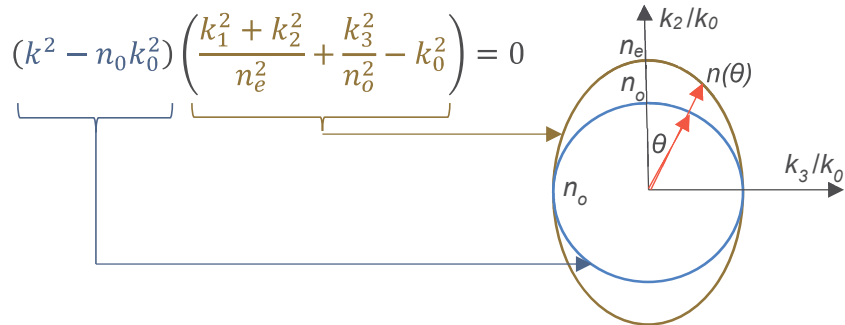


**Figure 2.12:** The  $k$  surface.

## Wave Plate (Retarder Plate)

The most basic application of an anisotropic materials is a **wave plate** or **retarder plate**, cut from a slice of uniaxial crystal with the optical axis oriented vertically in the plane of the plate (Figure 2.13). It is an optical element that produces some retardation between the orthogonal components of the wave. Light travelling through the plate will be delayed based on its polarization, the vertical polarization component will experience a refractive index  $n_e$ , and the horizontal polarization component will experience a refractive index  $n_o$ . However, because the beam is traveling perpendicular to the optical axis, the extraordinary ray doesn't suffer any deflection. For a plate thickness  $d$ , the relative phase delay between the two polarizations is:

$$\delta = \frac{2\pi(n_e - n_o)}{\lambda} d = \frac{2\pi\Delta n}{\lambda} d \quad (2.33)$$

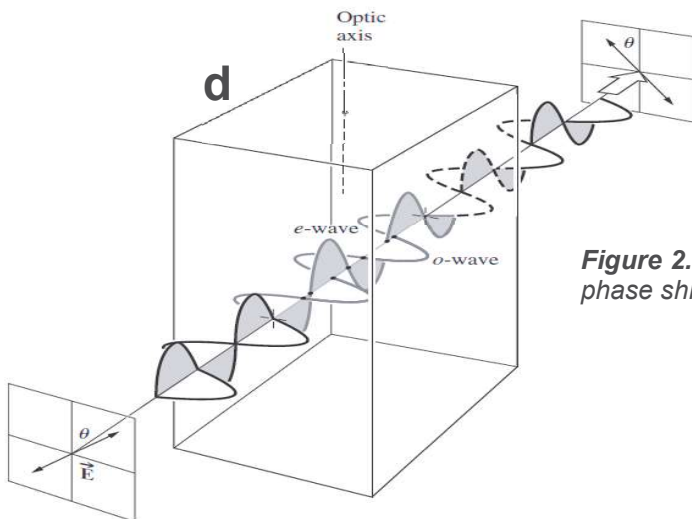


**Figure 2.13:** A half-wave plate showing how a net phase shift accumulates with the retarder.

where  $\lambda$  is the wavelength of light in the vacuum. By simply controlling the thickness of the plate, a variety of useful devices can be made.

## Fast Axis and Slow Axis

Just as a linear polarizer has a particular transmission axis, so we can define two transmission axes perpendicular to the propagation direction for a wave plate. These are known as the **fast axis** and **slow axis**, corresponding to the wave speeds of the transmitted orthogonal components (Figure 2.14). Thus, the phase of the wave along the fast axis is ahead of that along the slow axis. When  $n_e < n_o$ , as in calcite (negative uniaxial crystal), since  $v_e > v_o$  ( $c/n_e > c/n_o$ ) the extraordinary axis is aligned with the **fast axis** and the ordinary axis is called the **slow axis**. For  $n_e > n_o$  (positive uniaxial crystal), the situation is reversed. In other words, the so-called **slow ray** is the component for which the material has the higher effective refractive index (slower phase velocity), while the **fast ray** is the one with a lower effective refractive index (Figure 2.15).

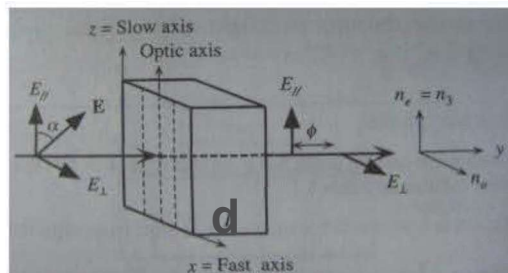


**Figure 2.14:** Retarder plate creates a phase difference between light polarized along the fast axis and light polarized along the slow axis.

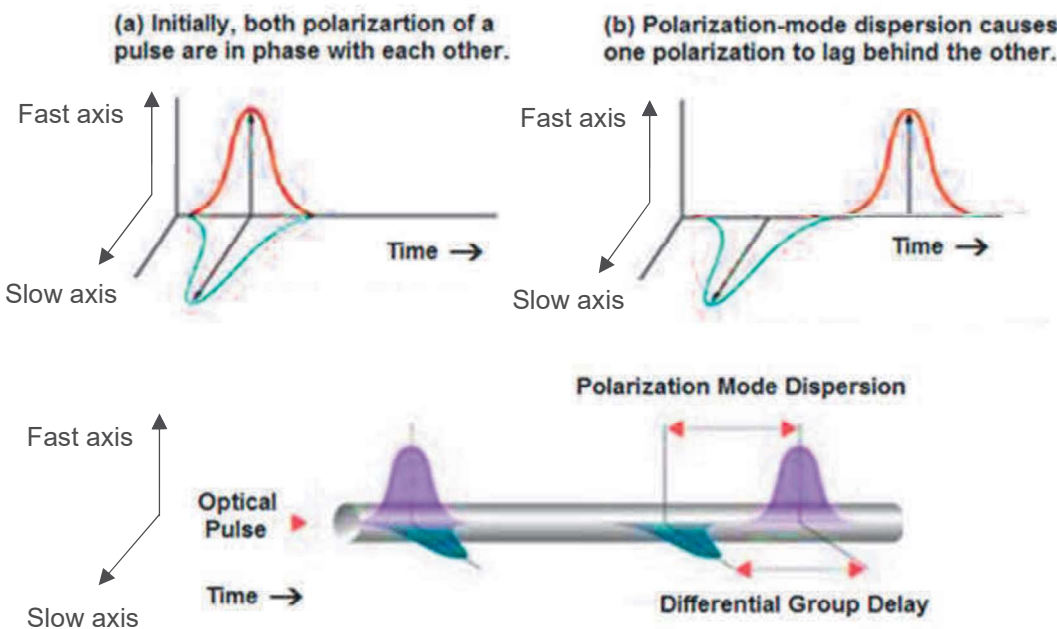


**Figure 2.15:** The concept of slow and fast axes and rays.

## 1/4-wave plate (quarter-wave plate)

A 1/4-wave plate (quarter-wave plate) is used to convert linear polarization to circular polarization and vice-versa. It delays one polarization by 90° relative to the other. In order to obtain circular polarization, the amplitudes of the two  $\mathbf{E}$  vector components must be equal and their phase difference must be 90° or 270°. A quarter-wave plate is capable of introducing a phase difference of 90° between the two components of incident light. The amplitudes of the two components will be equal only when the incident linear polarization direction makes an angle of 45° with respect to the optic axis of the crystal. The direction of polarization of the incident light with respect to the optic axis of the quarter-wave plate is equally important (Figure 2.16). Assume a linear polarizer at 45° in front of the 1/4-wave plate. The component of  $\mathbf{E}$  along the slow axis is retarded by one-quarter cycle or 90°. If the light beam after the first polarizer is described by

$$\frac{E_0}{\sqrt{2}} \cos(kz - \omega t) \hat{x} + \frac{E_0}{\sqrt{2}} \cos(kz - \omega t) \hat{y} \quad (2.34)$$

where  $\hat{x}$  and  $\hat{y}$  are the unit vector along the x- and y-axis, respectively, and  $k$  is with the wave vector. Then following the 1/2-wave plate, the field is

$$\frac{E_0}{\sqrt{2}} \cos(kz - \omega t) \hat{x} + \frac{E_0}{\sqrt{2}} \cos(kz - \omega t + 90^\circ) \hat{y} = \frac{E_0}{\sqrt{2}} \cos(kz - \omega t) \hat{x} + \frac{E_0}{\sqrt{2}} \sin(kz - \omega t) \hat{y}. \quad (2.35)$$

In an isotropic medium, for a (electric field vector) wavevector  $\mathbf{E}$

$$\mathbf{E}(\mathbf{r}, t) = \mathbf{E}_0 e^{i(\omega t - \mathbf{k} \cdot \mathbf{r})} \quad (2.36)$$

where  $\mathbf{E}_0$  is a Jones vector containing the details of the polarization. If the wave direction to be along the z-axis

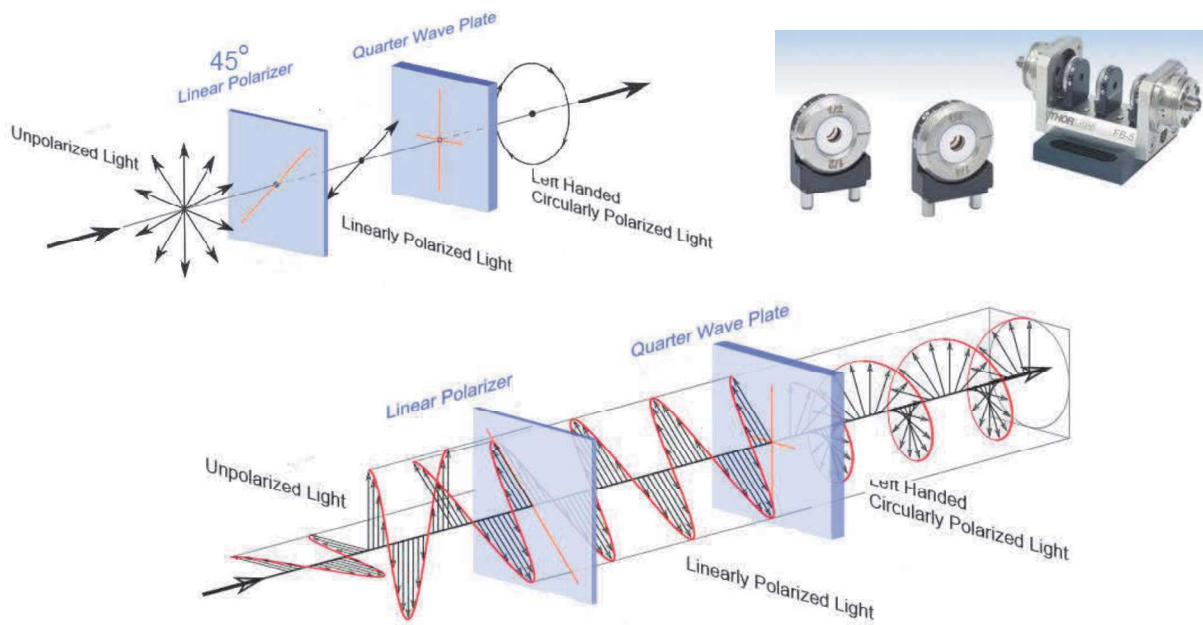


**Figure 2.16:** 1/4-wave plate (quarter-wave plate).

$$\mathbf{E}_0 = |E_0| \begin{bmatrix} \cos \theta \\ \sin \theta \end{bmatrix} \quad (2.37)$$

where  $\theta$  is the angle of  $\mathbf{E}_0$  relative to the x-axis. Therefore, for linearly x-polarized light  $\theta = 0$  and  $\mathbf{E}_0 = |E_0| \begin{bmatrix} 1 \\ 0 \end{bmatrix}$ , similarly, for linearly y-polarized light  $\theta = \pi/2$  and  $\mathbf{E}_0 = |E_0| \begin{bmatrix} 0 \\ 1 \end{bmatrix}$ .

For a quarter-wave plate, we have  $\delta = \pm\pi/2$ . The Jones matrix for a quarter-wave plate is given by

$$\mathbf{M} = \begin{bmatrix} 1 & 0 \\ 0 & \pm i \end{bmatrix} \quad (2.38)$$

After transmission through a quarter-wave plate the new polarization will be

$$\mathbf{E}_1 = |E_0| \begin{bmatrix} 1 & 0 \\ 0 & \pm i \end{bmatrix} \begin{bmatrix} \cos \theta \\ \sin \theta \end{bmatrix} = |E_0| \begin{bmatrix} \cos \theta \\ \pm i \sin \theta \end{bmatrix} \quad (2.39)$$

this yields elliptically polarized light. In this case, the principle axes of the ellipse are aligned with the  $E_x$  and  $E_y$  axes. In the specific case where  $\cos \theta = \sin \theta$  we have  $\theta = \pi/4$  and

$$\mathbf{E}_1 = \frac{1}{\sqrt{2}} |E_0| \begin{bmatrix} 1 \\ \pm i \end{bmatrix} \quad (2.40)$$

This is the Jones vector for circularly polarized light. Specifically, as given in the last section, for  $\delta = \pi/2$  we have right circular polarization and for  $\delta = -\pi/2$  we have left circular polarization.

Thus, a quarter-wave plate introduces a phase shift of  $\delta = \pi/2$  between the components of the optical field, producing elliptically polarized light. In the specific case where  $E_x$  and  $E_y$  are initially equal, the quarter waveplate produces circularly polarized light.

## 1/2-wave plate (half-wave plate)

A 1/2-wave plate inverts the phase of one polarization relative to the other. A half-wave plate functions as a polarization rotator for linearly polarized light. It rotates the polarization of a linearly polarized light by twice the angle between its optic axis and the initial direction of polarization. It introduces a phase difference of radians between the two components of the electric field vectors (Figure 2.17).

Let us imagine a linear polarizer at  $45^\circ$  in front of the 1/2-wave plate. The component of  $\mathbf{E}$  along the slow axis is retarded by one-half cycle or  $180^\circ$ . If the light beam after the first polarizer is described by

$$\frac{E_0}{\sqrt{2}} \cos(kz - \omega t) \hat{x} + \frac{E_0}{\sqrt{2}} \cos(kz - \omega t) \hat{y} \quad (2.41)$$

Then following the 1/2-wave plate, the field is

$$\frac{E_0}{\sqrt{2}} \cos(kz - \omega t) \hat{x} - \frac{E_0}{\sqrt{2}} \cos(kz - \omega t) \hat{y} \quad (2.42)$$

A half-wave plate, introduces a retardation of  $\delta = \pm\pi$ . The Jones matrix for a quarter-wave plate is given by

$$\mathbf{M} = \begin{bmatrix} 1 & 0 \\ 0 & -1 \end{bmatrix}. \quad (2.43)$$

After transmission through a half-wave plate the new polarization will be

$$\mathbf{E}_1 = |E_0| \begin{bmatrix} 1 & 0 \\ 0 & 1 \end{bmatrix} \begin{bmatrix} \cos \theta \\ \sin \theta \end{bmatrix} = |E_0| \begin{bmatrix} \cos \theta \\ -\sin \theta \end{bmatrix}. \quad (2.44)$$

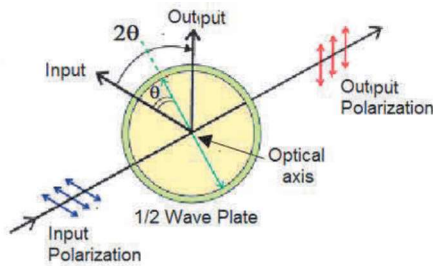


**Figure 2.17:** 1/2-wave plate (half-wave plate).

Thus, this has the effect of reversing the direction of y-component. In other words, the half-wave plate has the effect of rotating a state of linear polarization by  $-2\theta$  through the x-axis. Note that this is equivalent to a rotation of  $-2\theta'$  through the y-axis, where  $-\theta'$  is the angle of the electric field vector to the y-axis. Thus, whilst the fast axis may be aligned in either the x or y directions, we may say unambiguously that a half-wave plate has the effect of rotating a linear state of polarization by an angle  $-2\theta$  through the fast (or slow) axis, where  $\theta$  is the initial angle of the electric field vector to the fast (or slow) axis.

## Applications of Anisotropic Retarder Plates

Table 2.4 lists Jones vectors of various polarization states, wave plates and polarizers at selected orientations.

**Table 2.4:** Jones vectors of various polarization states.

	Linearly polarized with angle $\theta$ with x-axis	$\begin{bmatrix} \cos\theta \\ \sin\theta \end{bmatrix}$
	Left circularly polarized	$\frac{1}{\sqrt{2}} \begin{bmatrix} 0 \\ 1 \end{bmatrix}$
	Right circularly polarized	$\frac{1}{\sqrt{2}} \begin{bmatrix} 0 \\ 1 \end{bmatrix}$
	Linear polarizer with angle $\theta$ with x-axis <i>Transmission axis</i>	$\begin{bmatrix} \cos^2\theta & \cos\theta \sin\theta \\ \sin\theta \cos\theta & \sin^2\theta \end{bmatrix}$
	Waveplate with optical axis along x-axis <i>Optical axis</i>	$\begin{bmatrix} e^{-i\delta/2} & 0 \\ 0 & e^{i\delta/2} \end{bmatrix}$
	Waveplate with optical axis along y-axis <i>Optical axis</i>	$\begin{bmatrix} e^{i\delta/2} & 0 \\ 0 & e^{-i\delta/2} \end{bmatrix}$
	Waveplate with optical axis angle $45^\circ$ with x-axis <i>Optical axis</i>	$\begin{bmatrix} \cos(\delta/2) & -i \sin(\delta/2) \\ -i \sin(\delta/2) & \cos(\delta/2) \end{bmatrix}$
	Waveplate with optical axis angle $\theta$ with x-axis <i>Optical axis</i>	$\begin{bmatrix} e^{-i\delta/2}\cos^2\theta + e^{i\delta/2}\sin^2\theta & -i \sin(\delta/2)\sin 2\theta \\ -i \sin(\delta/2)\sin 2\theta & e^{-i\delta/2}\sin^2\theta + e^{i\delta/2}\cos^2\theta \end{bmatrix}$

Figure 2.18 indicates some facts about the wave plates.

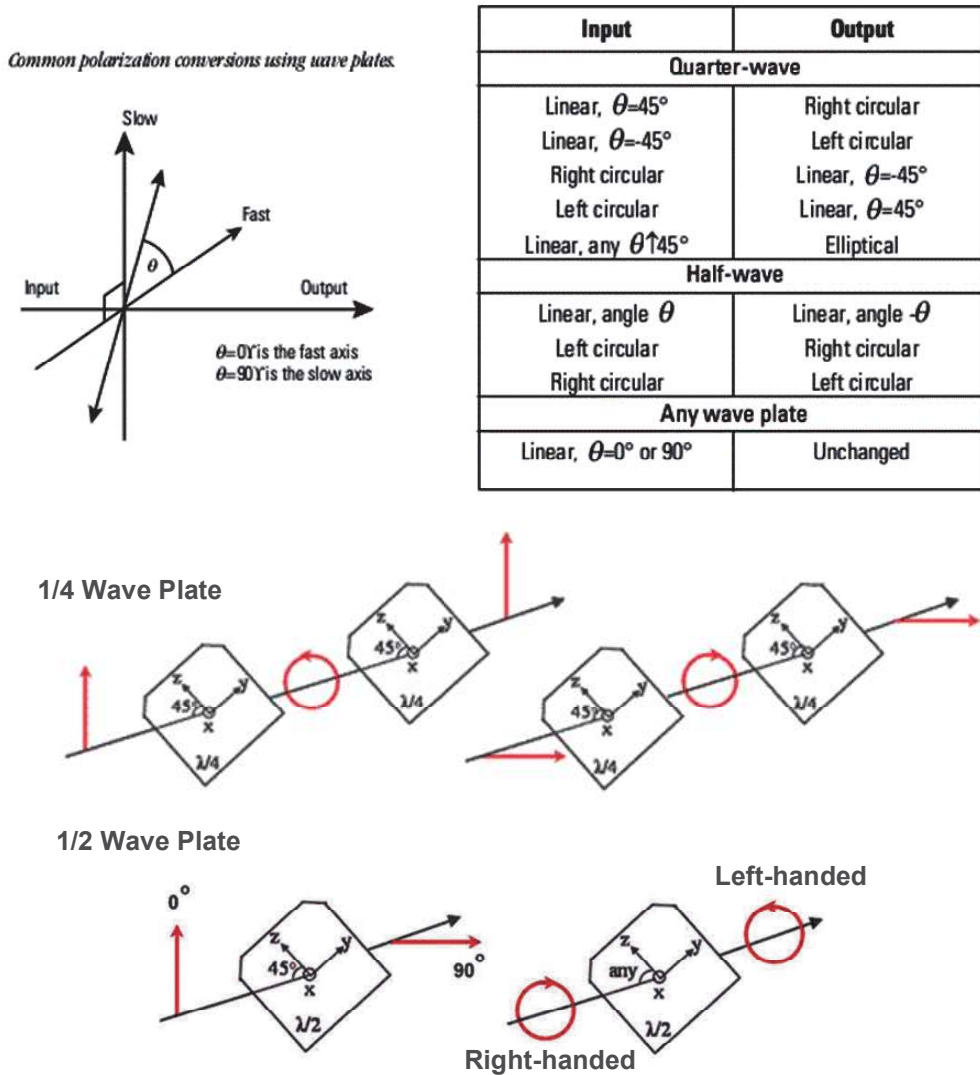


Figure 2.18: Some facts about the wave plates.

### A birefringent plate sandwiched between a pair of parallel polarizers

If a birefringent plate with thickness of  $d$  sandwiched between a pair of parallel polarizers – the axis of polarization for each polarizer is aligned in the same direction (Figure 2.19). and the plate is oriented so that the “slow” and “fast” axes are at  $45^\circ$  with respect to the transmission axes of polarizers, the Jones vector presentation of the electric field vector of the transmitted beam is

$$E = \begin{bmatrix} 0 & 0 \\ 0 & 1 \end{bmatrix} \begin{bmatrix} \cos(\delta/2) & -i \sin(\delta/2) \\ -i \sin(\delta/2) & \cos(\delta/2) \end{bmatrix} \frac{1}{\sqrt{2}} \begin{bmatrix} 0 \\ 1 \end{bmatrix} = \frac{1}{\sqrt{2}} \begin{bmatrix} 0 \\ \cos(\delta/2) \end{bmatrix} \quad (2.45)$$

where  $\delta = 2\pi(n_e - n_o)/d$ . Then, the transmitted beam (that passes through two parallel polarizers) is

$$I = E^2 = \frac{1}{2} \cos^2(\delta/2) = \frac{1}{2} \cos^2\left(\frac{2\pi(n_e - n_o)L}{d}\right). \quad (2.46)$$

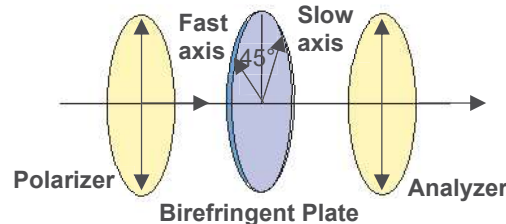


**Figure 2.19:** a birefringent plate sandwiched between a pair of parallel polarizers.

### A birefringent plate sandwiched between a pair of crossed polarizers

If a birefringent plate with thickness of  $d$  sandwiched between a pair of crossed polarizers (Figure 2.20), and the plate is oriented so that the “slow” and “fast” axes are at 45° with respect to the transmission axes of polarizers, the Jones vector presentation of the electric field vector of the transmitted beam is

$$E = \begin{bmatrix} 1 & 0 \\ 0 & 0 \end{bmatrix} \begin{bmatrix} \cos(\delta/2) & -i \sin(\delta/2) \\ -i \sin(\delta/2) & \cos(\delta/2) \end{bmatrix} \frac{1}{\sqrt{2}} \begin{bmatrix} 0 \\ 1 \end{bmatrix} = \frac{-i}{\sqrt{2}} \begin{bmatrix} \sin(\delta/2) \\ 0 \end{bmatrix}. \quad (2.47)$$

Therefore, the transmitted beam (that passes through two crossed polarizers) is

$$I = E^2 = \frac{1}{2} \sin^2(\delta/2) = \frac{1}{2} \sin^2\left(\frac{2\pi(n_e - n_o)L}{d}\right). \quad (2.48)$$

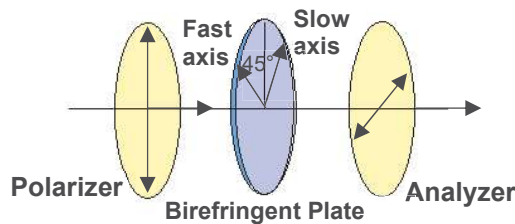


**Figure 2.20:** a birefringent plate sandwiched between a pair of crossed polarizers.

### A birefringent plate sandwiched between a pair of polarizers

If we rotate the analyzer so that the transmission axis of the analyzer form an angle  $\theta$  with respect to polarizer, then the input and output polarizers are neither parallel nor crossed and the plate is oriented so

that the "slow" and "fast" axes are at 45° with respect to the transmission axes of polarizers, the Jones vector presentation of the electric field vector of the transmitted beam is

$$\begin{aligned} E &= \begin{bmatrix} \cos^2\theta & \cos\theta \sin\theta \\ \sin\theta \cos\theta & \sin^2\theta \end{bmatrix} \begin{bmatrix} \cos(\delta/2) & -i \sin(\delta/2) \\ -i \sin(\delta/2) & \cos(\delta/2) \end{bmatrix} \frac{1}{\sqrt{2}} \begin{bmatrix} 0 \\ 1 \end{bmatrix} \\ &= \frac{-i \cos\theta \sin(\delta/2) + \sin\theta \cos(\delta/2)}{\sqrt{2}} \begin{bmatrix} \cos\theta \\ \sin\theta \end{bmatrix}. \end{aligned} \quad (2.49)$$

Therefore, the transmitted beam (that passes through two parallel polarizers) is

$$I = E^2 = \frac{1}{2} \cos^2\theta \sin^2\left(\frac{\delta}{2}\right) + \frac{1}{2} \sin^2\theta \cos^2\left(\frac{\delta}{2}\right). \quad (2.50)$$

## Finding the Fast and Slow Axes of a Retarder

There is a simple way to find the axes of a retardation plate. This requires two linear polarizers. Orient one linear polarizer so the axis is horizontal. Put the other linear polarizer in front of the first, oriented so that the axis is vertical. Place the retardation plate between the two crossed polarizers. Rotate only the retardation plate until maximum transmission is reached. The fast and slow axes will be at ±45° from horizontal.

To determine which axis is fast and which is slow, hold the retarder along one of the axes. For example, hold the plate by the left side and the right side. Rotate the retardation plate about this axis, so that the light is passing through a slightly thicker cross section of the retardation plate. Then repeat, using the other axis. If the color of the light changes from a bluish color to gray and then to black, then you are rotating about the fast axis. If the color changes from white to yellow and then to interference colors, then it is the slow axis.

## Determining ¼ Wave Retarder from ½ Wave Retarder

First, transmit linearly polarized light through the retarder. This light can either come from a light source that is already linearly polarized or be randomly polarized light that is sent through a linear polarizer. After the light is passed through the retarder, it can have one of two characteristics: if the retarder is ¼ wave, then the light is circularly polarized; if the retarder is ½ wave, then the light is linearly polarized, but at a different angle than the incident light.

Finally, you can use a second linear polarizer (typically called an "analyzer") to determine which retarder you possess. Place the analyzer in the path of the light coming from the retarder and rotate it. If, at certain angles of rotation, the light being emitted from the analyzer gets more intense and then is completely blocked out, you have a ½ wave retarder. If the light emitted is of similar intensity no matter how the analyzer is rotated, then you have a ¼ wave retarder. Please note that there are other types of retarders than ¼ wave and ½ wave, and this test does not take that into consideration.

# 3



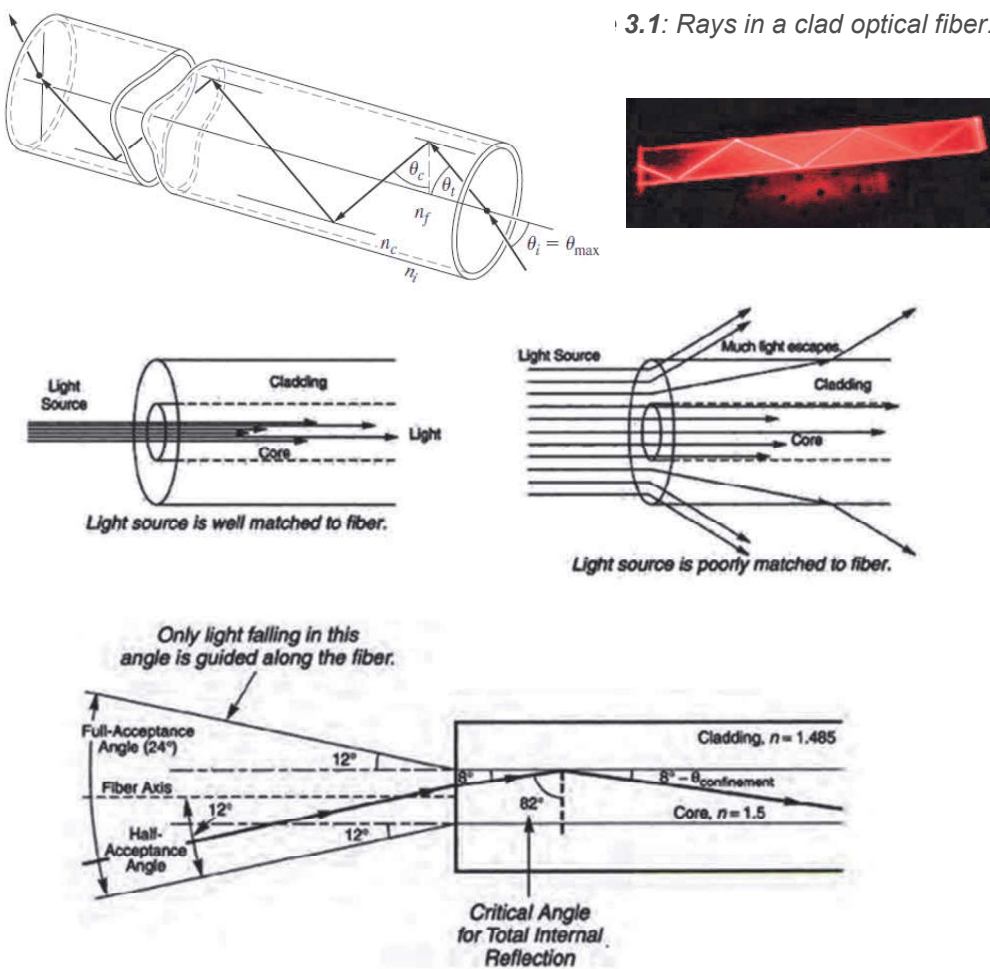
## PM Fiber

## Optical Fiber

In a fiber the core which carries the actual light signal surrounded by a transparent sheath glass **cladding** with a lower refractive index than the core that causes total internal reflection within the core (Figures 3.1 and 3.2). Typically, a fiber core might have an index ( $n_{\text{core}}$ ) of 1.62, and the cladding an index ( $n_{\text{cladding}}$ ) of 1.52, although a range of values is available. Notice that there is a maximum value  $\theta_{\max}$  of the incident angle  $\theta_i$ , for which the internal ray will impinge at the critical angle,  $\theta_c$ . Rays incident on the face at angles greater than  $\theta_{\max}$  will strike the interior wall at angles less than  $\theta_c = \sin^{-1}(n_{\text{core}}/n_{\text{cladding}})$ . They will be only partially reflected at each such encounter with the core-cladding interface and will quickly leak out of the fiber. Accordingly,  $\theta_{\max}$ , which is known as the acceptance angle, defines the half-angle of the acceptance cone of the fiber

$$\sin \theta_{\max} = \frac{1}{n_i} \sqrt{n_{\text{core}}^2 - n_{\text{cladding}}^2} \quad (3.1)$$

where  $n_i$  is the refractive index of the surrounding incident medium — such as air. The acceptance angle ( $2\theta_{\max}$ ) corresponds to the vertex angle of the largest cone of rays that can enter the core of the fiber.



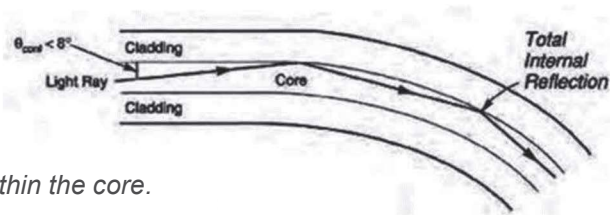


**Figure 3.2:** Total internal reflection within the core.

In a single-mode (SM) fiber, the core size is so small that it can only carry a single mode of light (Figure 3.3) – in a fiber with circular cross section, each mode has two independent states of polarization with the same propagation constant. Thus the fundamental mode in a single-mode fiber may be polarized in the x or y direction with the two orthogonal polarizations having the same propagation constant and the same group velocity. Since these polarization modes are strongly coupled, a tiny amounts of random birefringence in such a fiber, induced by strain, pressure, vibrations, and bending in the fiber, or variations in temperature will cause a tiny amount of crosstalk from one to the other polarization mode (Figure 3.4). However, a small coupling between the two polarization modes can lead to a large power transfer to one mode, completely changing the wave's net state of polarization. Since that coupling coefficient was unintended and a result of arbitrary stress or bending applied to fiber, the output state of polarization will itself be random, and will vary as those stresses or bends vary; it will also vary with wavelength. The result of this intrinsic instability is that the power distribution between the two modes, and therefore the output polarization orientation, is both random and time-varying. It is important to avoid the unwanted birefringence in a fiber.

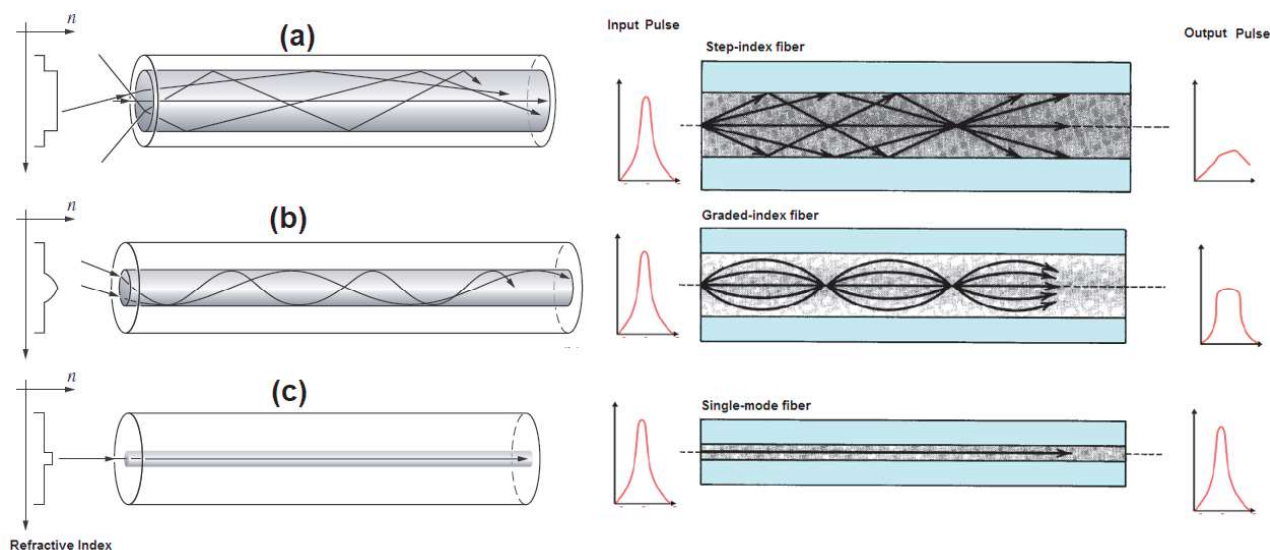


**Figure 3.3:** Geometry, refractive-index profile, and typical rays in: (a) a multimode step-index fiber, (b) a multimode graded-index fiber, and (c) a single-mode step-index fiber.

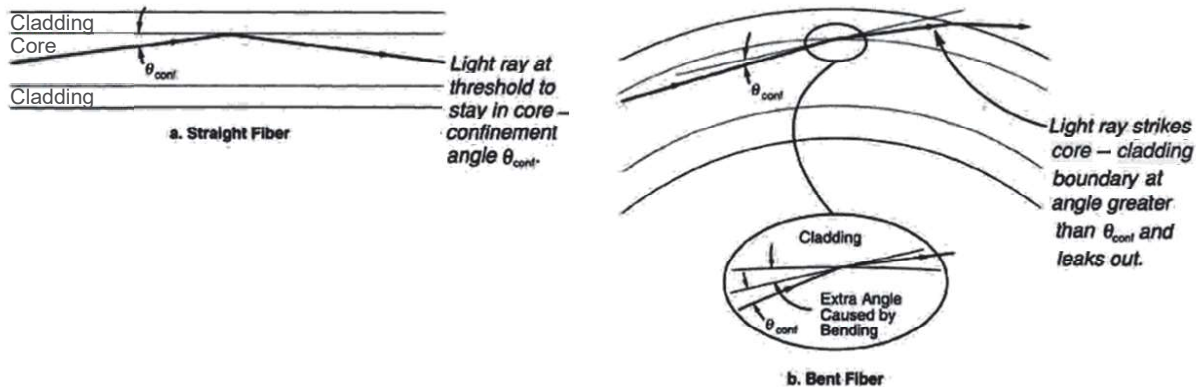


**Figure 3.4:** When the fiber is straight, light falls within its confinement angle. Bending the fiber changes the angle at which light hits the core-cladding boundary. If the bend is sharp, it hits the boundary at an angle outside the confinement angle and is refracted into the cladding where it can leak out.

## Polarization Maintaining (PM) Fiber

Polarization maintaining fiber generally resembles ordinary single-mode fiber in core and cladding diameters. It is constructed by using two asymmetric Stress-Applying Parts (SAP) at opposite sides of the core in the cladding of the fiber (see Figure 3.5). The core is placed in a uniform transverse mechanical stress field to induce a difference in index between orthogonal axes.

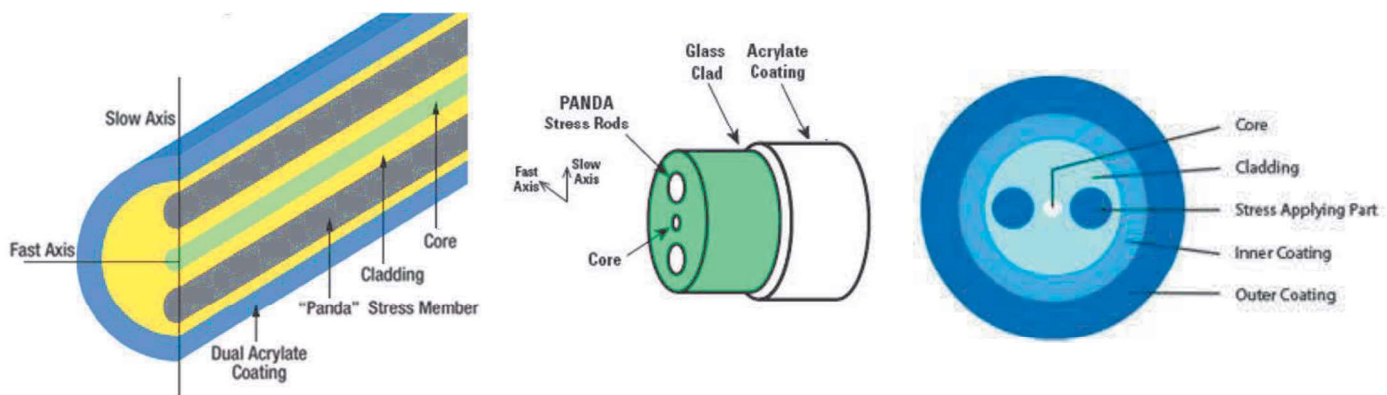


**Figure 3.5:** Panda Polarization Maintaining (PM) fiber.

In theory, there should be no exchange of power between the two polarization components. If the power of the light source is delivered into one polarization only, the power received remains in that polarization (Figure 3.6). In practice, however, slight random imperfections or uncontrollable strains in the fiber result in random power transfer between the two polarizations. This coupling is facilitated since the two polarizations have the same propagation constant and their phases are therefore matched. Thus linearly polarized light at the fiber input is transformed into elliptically polarized light at the output.

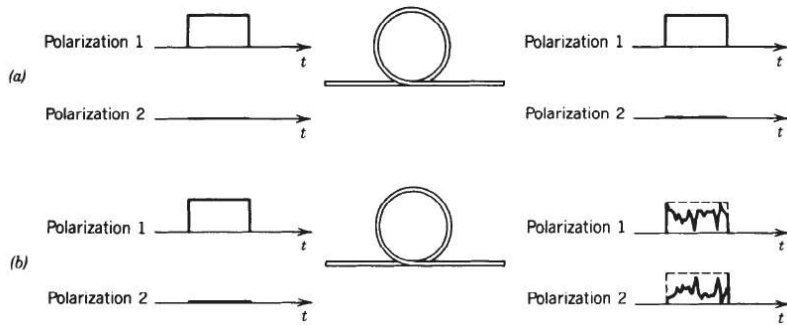


**Figure 3.6:** (a) Ideal polarization-maintaining fiber. (b) Random transfer of power between two polarizations.

In Polarization Maintaining (PM) Fiber, the stress changes the refractive index of the core due to photoelastic effect, seen by the modes polarized along the principal axes of the fiber, and results in birefringence. Therefore, no spurious mode is propagated through the SAPs, as long as the refractive index of the SAPs is less than or equal to that of the cladding (Figure 3.7). In other words, the basic propagation is still single mode but the induced birefringence means that the linear polarized modes are now weakly-coupled. The higher the birefringence, the weaker the coupling – so now, optical power launched into either of the two modes cannot switch (cross-couple) to the other, with the result that the polarization state of the transmitted light is preserved. To be more precise, SAPs force the light wave to follow a linear polarized controlled path (Figure 3.8).

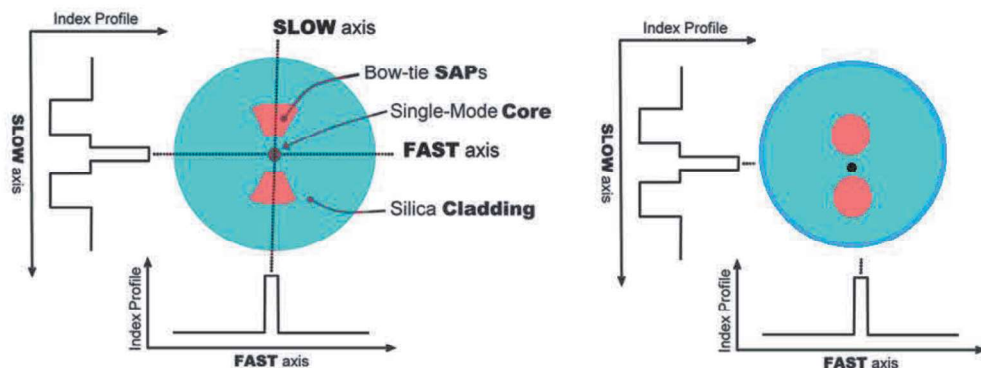
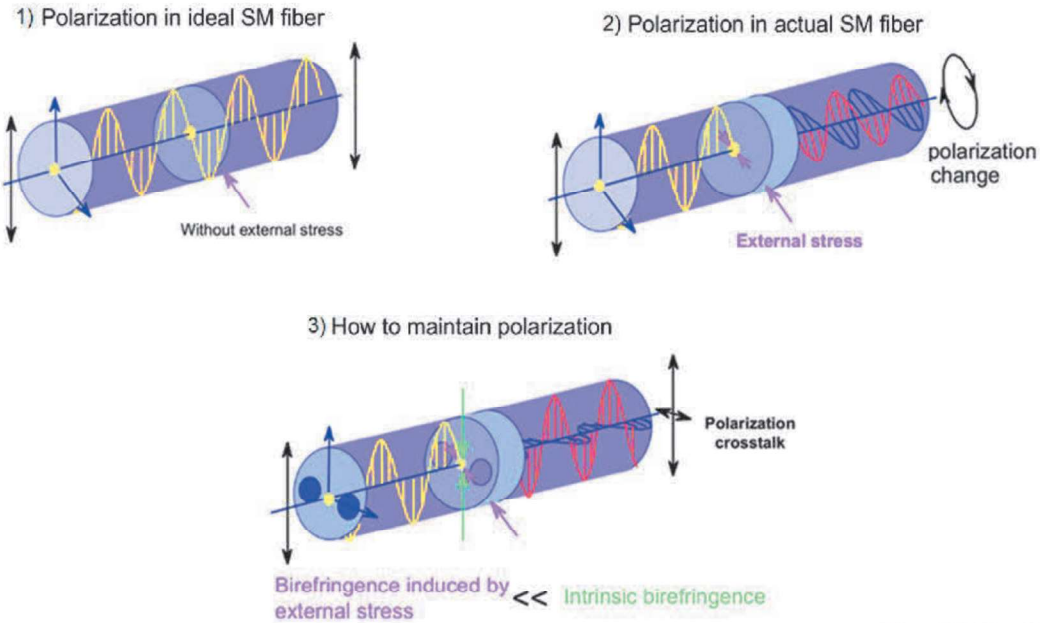


**Figure 3.7:** SAPs within the PM fiber.

SAPs creates a birefringence (double refraction) into the fiber which would cause the breaking of the circular symmetry of the fiber, thus creating the two principal transmission axes – **Fast axis** and **Slow axis** – within the fiber. In order to maintain a controlled linear polarization in a fiber-optic system, each component must be aligned on the desired transmission axis (Figure 3.9). The level of built-in stress is intended to be much higher than stresses produced by the application environment, so that the electric field of light launched along one of the principal (fast or slow) axes will remain aligned with that physical axis as it propagates.



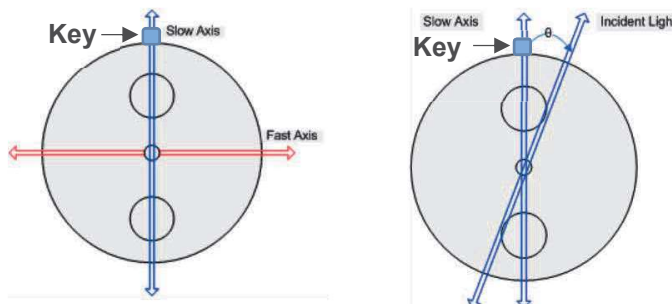
Copyright Fujikura Ltd.

**Figure 3.8:** Birefringence induced by SAPs within the PM fiber.

- The SAPs have different thermal expansion coefficient than that of the cladding material due to which an asymmetrical stress is applied on the fiber core after it is drawn from the preform and cooled down. When the fiber cools down at manufacturing the different thermal expansion coefficient of the SAPs creates stress along one axis of the core allowing for a highly birefringent fiber.

The slow axis alignment is the most popular in today technology. The better the polarized light is launched into either the fast or slow axis, the better the polarization is maintained and controlled within the system. But what is considered a good alignment? The importance of the PM fiber alignment leads to a polarization quality alignment measurement. The polarization extinction ratio (PER) measurement would provide such a measurement. Assuming that a perfectly linear polarized light wave is incident to a perfect fiber misaligned by an angle  $\theta$  with regards to the slow axis of the fiber (Figure 3.9), the *ER* can be expressed as:

$$ER \leq -10 \log(\tan 2\theta). \quad (3.2)$$

**Figure 3.9:** Fast and slow axes alignment.

A high extinction ratio is considered to be within 20 dB and 30 dB. Thus to achieve an extinction ratio of 20 dB, the misalignment should be less than 6° while for an extinction ratio of 30 dB, the misalignment should be less than 1.8°.

When an arbitrary beam of light strikes the surface of a birefringent material, the polarizations corresponding to the ordinary and extraordinary rays generally take somewhat different paths. There are two main aspects involving the PM alignment:

1. The first aspect deals with the quality of alignment of the optical sources in the system. The PM launch method helps align the light relative to a principal polarization state of a PM fiber optic cable. The way the laser is launched into the fiber is crucial to the total extinction ratio of the system and its overall performances. The light source must be highly polarized in order to avoid light being transmitted into both axes, making it impossible to predict the final polarization state of light.
2. The second aspect deals with maintaining this polarization throughout the whole system. Manufacturers offer lasers spliced into slow, fast or custom aligned connectorized fiber. It is crucial that the connector is aligned with its key and with the system's polarization axis.

Manufacturers offer pre-aligned (slow or fast axis) adjustable key connectors which can be in-system aligned (Figure 3.10). These connectors have a connector body which can be turned in order to obtain the highest ER possible. In order to achieve the highest ER measurement from a PM connectorized fiber optic system, several conditions must be met.

- First of all, the source light must be highly polarized and properly launched in the desired axis of the PM fiber.
- All over the system, the polarization of the light wave must also be aligned with the desired transmission axis.
- If the PM optical path is constructed by several segments of fiber (*i.e.* patch cords) joined together by optical connectors, the rotational alignment within the mating connectors and the connector choice are of the highest importance.

If all these requirements are met, polarized light which travels in the desired axis can be transmitted with up to 1000 times more power than in the “wrong” axis, therefore ensuring that the polarization maintenance is good throughout the entire system.

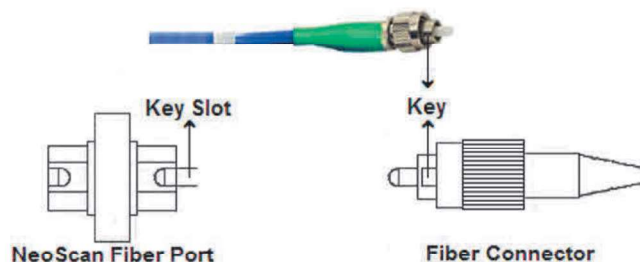


**Figure 3.10:** key connector of a PM fiber.

## PM Fiber Elements

A fiber optic cable contains one or many optic fibers which are covered by several protective layers and are used to transfer light signals. Optical fibers consist of glass or plastic cores in cladding tubes made of the same material; together, the core and the cladding tube are as thin as a human hair and the core is extremely clear that light signals can be perfectly transferred through it (Figure 3.11). A fiber optic core cannot possibly be handled on its own, which is why it is always surrounded by a color coded buffer tube. These optical fibers are usually reinforced by a strength element layer made of glass fibers or Kevlar, which is always covered by a protective color coded outer sheath jacket. A fiber optic cable usually consists of four elements:

1. Inner light transferring fibers, micrometers thin that consist of three layers:
  - i. The center core is the actual medium through which the light is transferred, and it has precisely selected characteristics to be extremely clear and efficient.
  - ii. Every optic fiber core has a cladding that provides a lower refractive index and ensures the light is reflected and kept inside the core. The cladding layer is always stuck to optic core and they cannot be separated by any hand tool.
  - iii. On the other hand, the third acrylic buffer layer of an optic fiber can be removed and it serves the purpose of basic protection and support and does not contribute to the light transfer process. In addition to that, the acrylic buffer is usually color coded to provide easier handling of multiple fiber optic cables, which might contain hundreds of fibers depending on the purpose of the cable.
2. The inner protective acrylic coating buffer tube, which can be a single loose tube that contains all the optical fibers loosely inside of it. This can be removed and it serves the purpose of basic protection and support and does not contribute to the light transfer process
3. The strength element has a lot of material options like braids of Kevlar or glass fiber or a metal armor, non-metal armor or gel; and has layout variations of grouping the fiber inner buffer tubes in single shells or multi-shells. The strength element layer determines the tension support of the cable and flexibility, and it is used to determine the built of the fiber optic cable; whether it is tight, semi-tight, loose, armored or water resistant.

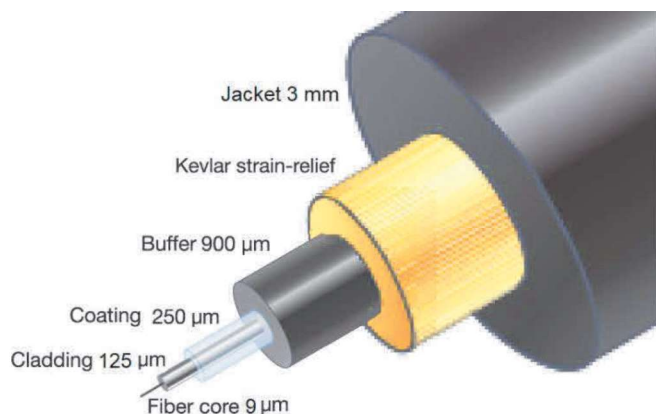


**Figure 3.11: Cross section of Panda PM fiber.**

4. The protective outer sheath jacket that mainly protects the fiber optic cable from the conditions of the surrounding environment. If the cable is made for outdoor usage it can be resistant to UV sun rays, water, pressure and tension; and if it was made for indoor usage it is usually very reflexive and has a high performance.

These four elements that establish one fiber optic cable may be a bit different from one cable type to another, from one manufacturer to another and they are different also according the type of the intended termination point or connector of the fiber optic cable; which means the possibilities with fiber optic cables is limitless and live up to the hype and connection speeds they are made for.

## Optical Fiber Core Dimensions

Because the core and cladding are always together as one unit, the measurement standard is always determined by the diameter value of both elements as a ratio in micro meters (Figure 3.12). The main core and cladding standards are 62.5/125 $\mu\text{m}$  or 50/125 $\mu\text{m}$  for multi-mode fibers and 9/125 $\mu\text{m}$  for single-mode and PM fibers. The outer acrylic is variable and the manufacturer can choose its thickness and color. The below illustration demonstrates a section of one fiber of all three standards.

For PM Fibers:

- Core diameter: 9  $\mu\text{m}$
- Cladding diameter: 125  $\mu\text{m}$
- Coating diameter: 250  $\mu\text{m}$  or 400  $\mu\text{m}$  – we use 250  $\mu\text{m}$
- Buffer diameter: 500  $\mu\text{m}$  or 900  $\mu\text{m}$  – we use 900  $\mu\text{m}$  white Polyester-elastomer coating
- Jacket Polyester-elastomer/Polyolefin coating outer diameter (OD): 1 mm or 3 mm – we use 3 mm OD.

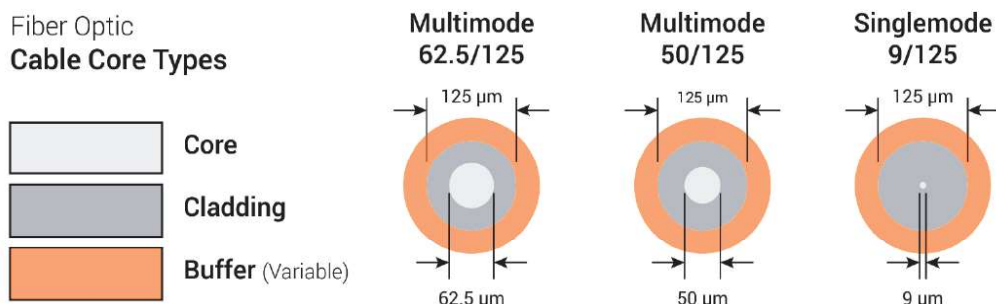


*Figure 3.12: The core dimension of optical fiber.*

## Fiber Optic Connector Types

**SMA:** due to its stainless steel structure and low-precision threaded fiber locking mechanism, this connector is used mainly in applications requiring the coupling of high power laser beams into large-core multimode fibers. Typical applications include laser beam delivery systems in medical, bio-medical, and industrial applications. The typical insertion loss of an SMA connector is greater than 1 dB (Figure 3.13).

**ST:** The ST connector is used extensively both in the field and in indoor fiber optic LAN applications. Its high-precision, ceramic ferrule allows its use with both multimode and single-mode fibers. The bayonet style, keyed coupling mechanism featuring push and turn locking of the connector, prevents over tightening and damaging of the fiber end. The insertion loss of the ST connector is less than 0.5 dB, with typical values of 0.3 dB being routinely achieved.

**FC:** The FC has become the connector of choice for single-mode and PM fibers and is mainly used in fiber-optic instruments, SM fiber optic components, and in high-speed fiber optic communication links. This high-precision, ceramic ferrule connector is equipped with an anti-rotation key, reducing fiber endface damage and rotational alignment sensitivity of the fiber. The key is also used for repeatable alignment of fibers in the optimal, minimal loss position. Multimode versions of this connector are also available. The typical insertion loss of the FC connector is around 0.3 dB.

**SC:** The SC connector is becoming increasingly popular in single-mode fiber optic telecom and analog CATV, field deployed links. The high-precision, ceramic ferrule construction is optimal for aligning single-mode optical fibers. The connectors' outer square profile combined with its push-pull coupling mechanism, allow for greater connector packaging density in instruments and patch panels. The keyed outer body prevents rotational sensitivity and fiber end face damage. Multimode versions of this connector are also available. The typical insertion loss of the SC connector is around 0.3 dB.

**LC:** LC is a newer design connector that uses a 1.25 mm ferrule, half the size of the ST. Otherwise, it's a standard ceramic ferrule connector, easily terminated with any adhesive. Good performance, highly favored for single mode.



*Figure 3.13: Fiber Optic Connector Types.*

## Fiber Optic Endface

Once the optical fiber is terminated with a particular connector, the connector endface preparation will determine what the connector return loss, also known as back reflection, will be (Figure 3.14). The back reflection is the ratio between the light propagating through the connector in the forward direction and the light reflected back into the light source by the connector surface. The return loss can be attributed to:

- Backscattering:
  - When the density fluctuations in the fiber core lead to density fluctuations of the refractive index (Rayleigh Scattering);
  - When imperfections at the core and cladding interface acts as a source of scattering.

- Fresnel reflection: occur when there is an abrupt change in the density of the transmission media. An example is when light ray passes from fiber core to air then back to the fiber core (connectors) or when light ray passes from fiber core to index matching gel then back to the fiber core (mechanical splice).

Minimizing back reflection is of great importance in high-speed and analog fiber optic links, utilizing narrow line width sources such as DFB lasers, which are prone to mode hopping and fluctuations in their output (Figure 3.15).

**Flat Polish:** A flat polish of the connector surface will result in a back reflection of about -16 dB (4%).

**PC Polish:** The Physical Contact (PC) polish results in a slightly curved connector surface, forcing the fiber ends of mating connector pairs into physical contact with each other. This eliminates the fiber-to-air interface, thereby resulting in back reflections of -30 to -40 dB. The PC polish is the most popular connector endface preparation, used in most applications.

**SPC and UPC Polish:** in the Super PC (SPC) and Ultra PC (UPC) polish, an extended polishing cycle enhances the surface quality of the connector, resulting in back reflections of -40 to -55 dB and < -55 dB, respectively. These polish types are used in high-speed, digital fiber optic transmission systems.

**APC Polish:** the Angled PC (APC) polish, adds an 8 degree angle to the connector endface. Back reflections of <-60 dB can routinely be accomplished with this polish.

In AFC connectors any light that is redirected back towards the source is actually reflected out into the fiber cladding, again by the virtue of the 8°angled end-face (Figure 3.15). APC connector back reflection does not degrade with repeated matings/unmatings. APC fiber connector can only be used with PM and single-mode fiber.

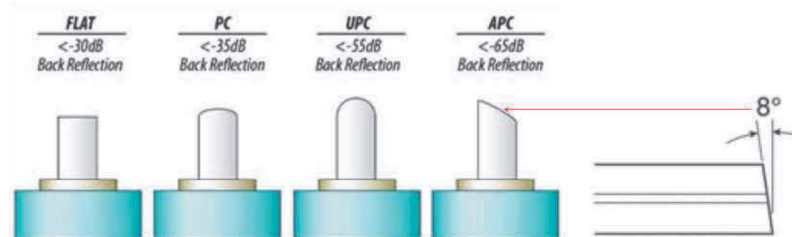


**Figure 3.14: Fiber Optic Connector Endface.**

## Fiber Preparation

**Fiber Cleaving** is the fastest way to achieve a mirror-flat fiber end — it takes only seconds. The basic principle involves placing the fiber under tension, scribing with a diamond or carbide blade perpendicular to the axis, and then pulling the fiber apart to produce a clean break.

**Fiber Stripping:** The outer sheath of fiber cables (jacket) can be removed using electrical cable stripping tools, and scissors or a razor blade can trim the Kevlar strength member. However, the fiber coating must be very carefully removed to avoid damaging the fiber — surface flaws and scratches are the cause of most fiber failures. The coating can be removed using our Fiber Optic Strippers.

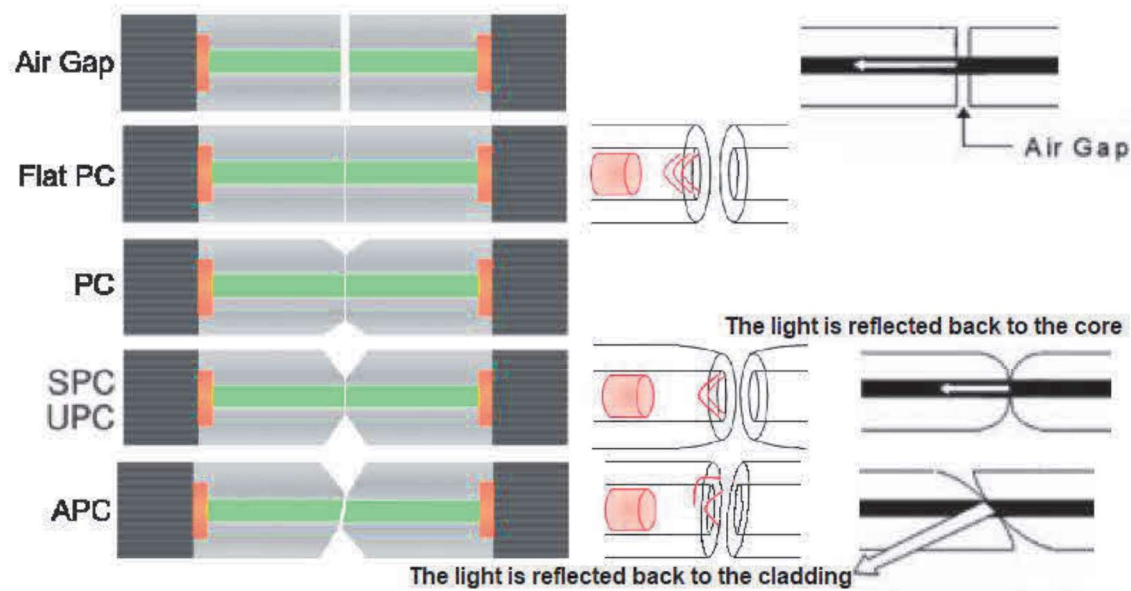
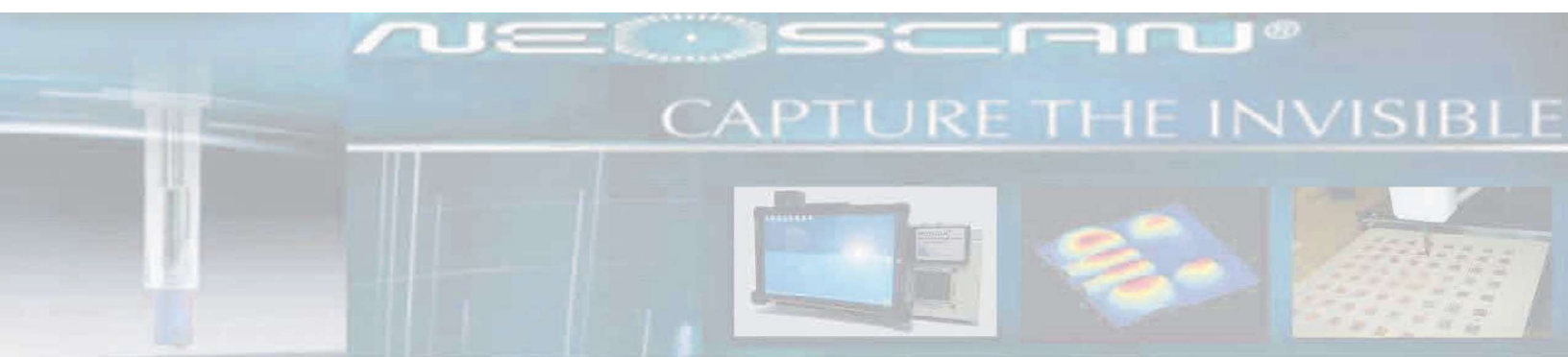


*Figure 3.15: The light reflection on the Fiber Optic Connector Endface.*

**Fiber Termination:** End surface quality is one of the most important factors affecting fiber connector and splice losses. Quality endfaces can be obtained by polishing or by using a fiber cleaver. Polishing is employed in connector terminations when the fiber is secured in a ferrule by epoxy.

# 4



## Pockels Effect

## Electro-Optic Effect in Crystals

The electro-optic effect is, loosely speaking, the change in the extraordinary and ordinary refractive indices ( $n_e$  and  $n_o$ ) resulting from the application of a DC or low-frequency electric field (Figure 4.1). For instance, in Kerr effect, an isotropic transparent substance becomes birefringent when placed in an electric field  $\mathbf{E}$ . The medium takes on the characteristics of a uniaxial crystal whose optic axis corresponds to the direction of the applied field. The two indices – parallel and perpendicular to the applied electric field – are associated with the two orientations of the plane-of-vibration of the wave. Their difference,  $\Delta n$ , is the birefringence, is proportional to the square of the field

$$\Delta n = n_e - n_o = \lambda_0 K E^2 \quad (4.1)$$

where  $K$  is the Kerr constant. The Pockels Effect is a linear electro-optical effect, inasmuch as the induced birefringence is proportional to the first power of the applied field

$$\Delta n = n_e - n_o = \lambda_0 K' E \quad (4.2)$$

and therefore the applied voltage ( $K'$  is a constant). The Pockels Effect exists only in certain crystals that lack a center of symmetry – in other words, crystals having no central point through which every atom can be reflected into an identical atom.

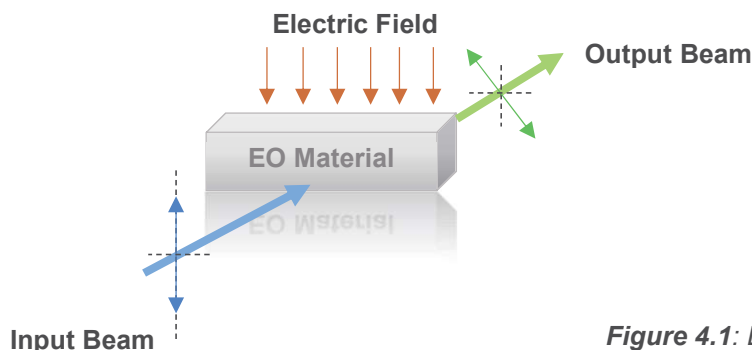


**Figure 4.1:** EO modulation of an optical signal.

## Nonlinear Effects

The usual classical treatment of the propagation of light—superposition, reflection, refraction, and so forth—assumes a linear relationship between the electromagnetic light field and the responding atomic system constituting the medium. But just as an oscillatory mechanical device (e.g., a weighted spring) can be overdriven into nonlinear response through the application of large enough forces, so too we might anticipate that an extremely intense beam of light could generate appreciable nonlinear optical effects.

Quite obviously in the extreme case of very high fields, we can expect that  $P$  will become saturated; in other words, it simply cannot increase linearly indefinitely with  $E$  (just as in the familiar case of ferromagnetic materials, where the magnetic moment becomes saturated at fairly low values of  $H$ ). Thus we can anticipate a gradual increase of the ever-present, but usually insignificant, nonlinearity as  $E$  increases. Since the directions of  $\vec{P}$  and  $\vec{E}$  coincide in the simplest case of an isotropic medium, we can express the polarization more effectively as

$$P_i = \sum_j \epsilon_0 \chi_{ij} E_j + \sum_j \sum_k \epsilon_0 \chi_{ijk} E_j E_k + \sum_j \sum_k \sum_l \epsilon_0 \chi_{ijkl} E_j E_k E_l + \dots \quad (4.3)$$

This shows that (for example), the product of any pair of field components  $E_j$  and  $E_k$  can contribute to  $P_i$  through a third-rank susceptibility tensor whose elements are  $\chi_{ijk}$ . The first point to note is that the higher-order terms normally get progressively smaller, so that the elements  $\chi_{ij}$  are the dominant factors determining the dielectric constant. The importance of the higher-order terms lies in a number of new and entirely different effects they make possible.

Consider, for example, an optical field (say, in the x-direction), which at any point can be described as  $E_x = E_0 \sin \omega t$  is incident on the medium. The resulting electric polarization

$$\begin{aligned} P_x &= \varepsilon_0 \chi_1 E_x + \varepsilon_0 \chi_2 E_x^2 + \varepsilon_0 \chi_3 E_x^3 + \dots = \varepsilon_0 \chi_1 E_0 \sin \omega t + \varepsilon_0 \chi_2 E_0^2 \sin^2 \omega t + \varepsilon_0 \chi_3 E_0^3 \sin^3 \omega t + \dots \\ &= \varepsilon_0 \chi_1 E_0 \sin \omega t + \frac{1}{2} \varepsilon_0 \chi_2 E_0^2 (1 - \cos 2\omega t) + \frac{1}{4} \varepsilon_0 \chi_3 E_0^3 (3 \sin \omega t - \sin 3\omega t) + \dots \end{aligned} \quad (4.4)$$

$P_x$  now has a contribution at an angular frequency  $2\omega$ ,  $3\omega$  ... i.e. second, third ... harmonic generation, because this component of  $P$  can be arranged to generate a new wave at the doubled or tripled frequency. However, the usual linear susceptibility,  $\chi_1$ , is much greater than the coefficients of the nonlinear terms  $\chi_2$ ,  $\chi_3$ , and so on, and hence the latter contribute noticeably only at high-amplitude fields. In other words, merely having a significant value of the appropriate coefficient  $\chi_{ijk}$  is not a sufficient condition for a strong second or third harmonic wave – a further requirement is that the phase velocities of the waves must be matched. As the harmonic light wave sweeps through the medium, it creates what might be thought of as a polarization wave, that is, an undulating redistribution of charge within the material in response to the field. If only the linear term were effective, the electric polarization wave would correspond to an oscillatory current following along with the incident light. The light thereafter reradiated in such a process would be the usual refracted wave generally propagating with a reduced speed  $v$  and having the same frequency as the incident light. In contrast, the presence of higher-order terms implies that the polarization wave does not have the same harmonic profile as the incident field. It is interesting to note that terms  $\varepsilon_0 \chi_1 E_0 \sin \omega t + 1/2 \varepsilon_0 \chi_2 E_0^2 (1 - \cos 2\omega t) + 1/4 \varepsilon_0 \chi_3 E_0^3 (3 \sin \omega t - \sin 3\omega t) + \dots$  can be likened to a Fourier series representation of the distorted profile of  $P(t)$ .

Now consider a situation when the field components are associated with different sources. For example, we might have  $E_x = E_{\text{optical}} e^{j\omega_o t}$  a component of an optical field and  $E_y = E_{\text{electrical}} e^{j\omega_s t}$  a field of much lower frequency derived from an external source such as a signal generator or a DC electric field. In this case, the new contribution to the polarization is

$$P_x = \varepsilon_0 \chi_{xxy} E_{\text{optical}} E_{\text{electrical}} e^{j(\omega_o + \omega_s)t}. \quad (4.5)$$

It appears that  $\chi_{xxy}$  has effectively been replaced by  $\chi_{xxy} + \chi_{xxy} E_{\text{electrical}} e^{j\omega_s t}$ . Thus, the dielectric constant has now become a function of the applied low-frequency field  $E_{\text{electrical}}$ . Keep in mind that  $E = E_{\text{optical}}(\omega) + E_{\text{electrical}}$ , and the second order nonlinear effect includes  $E_{\text{electrical}}^2$ ,  $E_{\text{optical}}^2(\omega)$ , as well as  $E_{\text{optical}}(\omega)E_{\text{electrical}}$  terms, however  $E_{\text{electrical}} \gg E_{\text{optical}}(\omega)$ . More generally

$$\chi_{ij}(E) = \chi_{ij} + \sum_k \chi_{ijk} E_k + \sum_k \sum_l \chi_{ijkl} E_k E_l + \dots \quad (4.6)$$

and  $1 + \chi = n^2$  with impermeability

$$\eta = \frac{\varepsilon_0}{\varepsilon} = \frac{1}{n^2}. \quad (4.7)$$

if the intensity of the electric field is small,  $\eta_{ij}(E)$  may be expanded in a Taylor's series about  $E=0$ :

$$\eta_{ij}(E) = \eta_{ij}(0) + \sum_k r_{ijk} E_k + \sum_k \sum_l s_{ijkl} E_k E_l + \dots \quad (4.8)$$

where

$$r_{ijk} = \frac{\partial \eta_{ij}}{\partial E_k} \Big|_{E=0} \quad (4.9)$$

are the linear Pockels coefficients – the first derivation of impermittivity tensor for zero electric field and

$$S_{ijkl} = \frac{1}{2} \frac{\partial^2 \eta_{ij}}{\partial E_k \partial E_l} \Big|_{E=0} \quad (4.10)$$

are the quadratic Kerr coefficients – the second derivation of impermittivity tensor for zero electric field. The changes of refractive index due the applied electric field  $E$  on electro-optical crystal is

$$\Delta n = n(E) - n_0 = \frac{\partial n}{\partial \eta} \Delta \eta = \left( -\frac{n^3}{2} \right) \Delta \eta = -\frac{1}{2} r n^3 E - \frac{1}{2} s n^3 E^3 + \dots \quad (4.11)$$

with  $\Delta \eta = rE + sE^2$

$$\Delta n = -\frac{1}{2} r n^3 E - \frac{1}{2} s n^3 E^3 + \dots \quad (4.12)$$

(see Figure 4.2). The Pockels effect can be observed only for materials without center of symmetry. Most common crystals used as Pockels cells are LiNbO<sub>3</sub>, LiTaO<sub>3</sub>, ADP (NH<sub>4</sub>H<sub>2</sub>PO<sub>4</sub>), KDP (KH<sub>2</sub>PO<sub>4</sub>). Typical values for Pockels coefficient  $r$  is 10<sup>-12</sup> to 10<sup>-10</sup> m/V. This means, for  $E = 106$  V/m the typical refractive index change ( $\Delta n$ ) is very small and it is of order from 10<sup>-6</sup> to 10<sup>-4</sup> for crystals (Table 4.1). For materials with center of symmetry, as gases, liquids, and certain crystals,  $n(E)$  must be an even function and Pockels coefficient must be equal to zero.

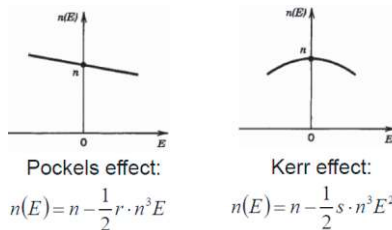


**Figure 4.2: Pockels and Kerr effects.**

All materials display the Kerr effect, with varying magnitudes, but it is generally much weaker than the Pockels effect, so only for centrosymmetric materials quadratic effect is not negligible. Typical values for Kerr coefficient  $s$  is 10<sup>-18</sup> to 10<sup>-14</sup> m/V<sup>2</sup> in crystals; 10<sup>-22</sup> to 10<sup>-19</sup> m/V<sup>2</sup> in liquids. So for  $E = 106$  V/m index change ( $\Delta n$ ) is very small 10<sup>-6</sup> to 10<sup>-2</sup> for crystals and 10<sup>-10</sup> to 10<sup>-7</sup> in liquids (Table 4.1).

**Table 4.1:** Pockels coefficient (left) and Kerr coefficient (right) for selected materials.

Material (wavelength if not 633 nm)	Linear electro-optic coefficient <sup>a</sup> $r$ (pm/V)	Refractive index $n_0$	Material ( $\lambda = 589$ nm, RT)	$s$ (pm/V <sup>2</sup> )
KH <sub>2</sub> PO <sub>4</sub> (KDP)	11	1.51	Nitrogen (STP)	$4 \times 10^{-6}$
KD <sub>2</sub> PO <sub>4</sub> (KD*P)	24.1	1.51	Glass (typical)	0.001
(NH <sub>4</sub> ) <sub>2</sub> PO <sub>4</sub> (ADP) $\lambda = 0.546$ nm	8.56	1.48	Carbon disulfide (CS <sub>2</sub> )	0.036
LiNbO <sub>3</sub> (lithium niobate)	30.9	2.29	Water (H <sub>2</sub> O)	0.052
LiTaO <sub>3</sub> (lithium tantalate)	30.5	2.18	Nitrotoluene (C <sub>7</sub> H <sub>7</sub> NO <sub>2</sub> )	1.4
GaAs (gallium arsenide) $\lambda = 10.6$ $\mu$ m	1.51	3.3	Nitrobenzene (C <sub>6</sub> H <sub>5</sub> NO <sub>2</sub> )	2.4
ZnS (zinc sulfide) $\lambda = 0.6$ $\mu$ m	2.1	2.36		
Quartz	1.4	1.54		

## Symmetry in Pockels and Kerr coefficients

Considering the expansion  $\chi_{ij} + \sum_k \chi_{ijk} E_k + \sum_k \sum_l \chi_{ijkl} E_k E_l$ , the tensor  $\chi_{ijk}$  describing the electro-optic effect will have a total of 27 elements (for each of the three possible directions of the polarization  $P_i$  there will be three directions for the field  $E_j$  and three for the field  $E_k$ ). However, the argument that showed that the dielectric tensor must be symmetric (so that  $\varepsilon_{ij} = \varepsilon_{ji}$  and  $\chi_{ij} = \chi_{ji}$ ) can also be shown to lead to  $\chi_{ijk} = \chi_{jik}$ . Thus, the number of different elements needed is only 18. However, the  $\chi_{ijk}$  terms themselves are not normally used to characterise the effect. Since they modify the polarization (and hence the dielectric constant), we expect that the presence of an external electric field will alter the shape of the index indicatrix. It is these changes that are traditionally used instead. Similarly, in expansion  $\eta_{ij}(0) + \sum_k r_{ijk} E_k + \sum_k \sum_l s_{ijkl} E_k E_l$ , in general,

- $\eta_{ij}(0)$  has  $3^2 = 9$  elements,
- $\{r_{ijk}\}$  has  $3^3 = 27$  elements,
- $\{s_{ijkl}\}$  has  $3^4 = 81$  elements.

Because  $\eta_{ij}$  is symmetric  $\eta_{ij} = \eta_{ji}$ , therefore,

- $\eta_{ij}(0)$  should have 6 independent elements,
- $\{r_{ijk}\}$  should have  $6 \times 3 = 18$  independent elements (since  $r_{ijk} = r_{jik}$ , and  $s_{ijkl} = s_{jikl}$ ),
- $\{s_{ijkl}\}$  should have  $6 \times 6 = 36$  independent elements ( $s_{ijkl} = s_{ijlk}$ ).

It is conventional to rename the pair of indices (Table 4.2):

- $(i, j)$ ,  $i, j = 1, 2, 3 \rightarrow$  as a single index  $I = 1, 2, \dots, 6$ .
- $(k, l)$ ,  $k, l = 1, 2, 3 \rightarrow$  as a single index  $K = 1, 2, \dots, 6$ .

In other words,  $r_{ijk} \rightarrow r_{Ik}$  is a  $6 \times 3$  matrix and  $s_{ijkl} \rightarrow s_{IK}$  is a  $6 \times 6$  matrix:

$$\begin{bmatrix} (i,j) \\ xx & xy & xz \\ yx & yy & yz \\ zx & zy & zz \end{bmatrix} \rightarrow \begin{bmatrix} I \\ 1 & 6 & 5 \\ 2 & 4 \\ 3 \end{bmatrix} \quad (4.13)$$

For example,  $r_{12k} \rightarrow r_{6k}$  and  $s_{1231} \rightarrow s_{65}$ . The notation 11 for  $xx$ , 12 for  $xy$  is also often employed. Hence,  $r_{yx}$  (which can also be written  $r_{231}$ ) becomes contracted to  $r_{41}$ . By symmetry, this is also equal to  $r_{321}$ . Similarly,  $r_{52}$  corresponds to  $r_{132}$  ( $= r_{312}$ ).

**Table 4.2:** Look up table for Index  $I$  that represents the pair of indices  $(i,j)$ .

$j$	$i : 1$	2	3
1	1	6	5
2	6	2	4
3	5	4	3

<sup>a</sup>The pair  $(i, j) = (3, 2)$ , for example, is labeled  $I = 4$ .

## Pockels Effect in Crystals

The electro-optic Pockels Effect describes the linear dependence of the refractive index on an applied field ( $\Delta n \propto E$ ). An electric field applied to certain crystals causes a slight change in the index of refraction, due to a redistribution of bond charges at the atomic level and possibly a slight deformation of the crystal lattice. In general, these alterations are not isotropic; that is, the changes vary with direction in the crystal. The net result is a change in the inverse dielectric constants (impermeability) tensor  $1/n_{ij}^2$  of the index ellipsoid in its general form:

$$\Delta\eta_{ij} = \Delta\left(\frac{\varepsilon_0}{\varepsilon_{ij}}\right) = \left(\frac{\varepsilon_0}{\varepsilon_{ij}}\right)_E - \left(\frac{\varepsilon_0}{\varepsilon_{ij}}\right)_{E=0} = \Delta\left(\frac{1}{n^2}\right)_{ij} = r_{ijk}E_k. \quad (4.14)$$

With the symmetric conditions<sup>1</sup>

$$\begin{bmatrix} \Delta\left(\frac{1}{n^2}\right)_1 \\ \Delta\left(\frac{1}{n^2}\right)_2 \\ \Delta\left(\frac{1}{n^2}\right)_3 \\ \Delta\left(\frac{1}{n^2}\right)_4 \\ \Delta\left(\frac{1}{n^2}\right)_5 \\ \Delta\left(\frac{1}{n^2}\right)_6 \end{bmatrix} = \begin{bmatrix} r_{11} & r_{12} & r_{13} \\ r_{21} & r_{22} & r_{23} \\ r_{31} & r_{32} & r_{33} \\ r_{41} & r_{42} & r_{43} \\ r_{51} & r_{52} & r_{53} \\ r_{61} & r_{62} & r_{63} \end{bmatrix} \begin{bmatrix} E_x \\ E_y \\ E_z \end{bmatrix}. \quad (4.15)$$

$E_x$ ,  $E_y$ , and  $E_z$  are the components of the applied electric field in principal coordinates. Thus, for example,  $\Delta(1/n_1^2) = r_{11}Ex + r_{12}Ey + r_{13}EZ$  and so on. The magnitude of  $\Delta(1/n^2)$  is typically on the order of less than  $10^{-5}$ . Therefore, these changes are mathematically referred to as perturbations.

The new impermeability tensor  $\tilde{\eta} = 1/\tilde{n}^2$  in the presence of an applied electric field is no longer diagonal in the reference principal dielectric axes system. It is given by

<sup>1</sup> An electric field applied in a general direction to any crystal, centrosymmetric or non-centrosymmetric, produces a quadratic change in the constants  $\Delta(1/n^2)$  due to the quadratic electro-optic effect according to

$$\begin{bmatrix} \Delta\left(\frac{1}{n^2}\right)_1 \\ \Delta\left(\frac{1}{n^2}\right)_2 \\ \Delta\left(\frac{1}{n^2}\right)_3 \\ \Delta\left(\frac{1}{n^2}\right)_4 \\ \Delta\left(\frac{1}{n^2}\right)_5 \\ \Delta\left(\frac{1}{n^2}\right)_6 \end{bmatrix} = \begin{bmatrix} S_{11} & S_{12} & S_{13} & S_{14} & S_{15} & S_{16} \\ S_{21} & S_{22} & S_{23} & S_{24} & S_{25} & S_{26} \\ S_{31} & S_{32} & S_{33} & S_{34} & S_{35} & S_{36} \\ S_{41} & S_{42} & S_{43} & S_{44} & S_{45} & S_{46} \\ S_{51} & S_{52} & S_{53} & S_{54} & S_{55} & S_{56} \\ S_{61} & S_{62} & S_{63} & S_{64} & S_{65} & S_{66} \end{bmatrix} \begin{bmatrix} E_x^2 \\ E_y^2 \\ E_z^2 \\ E_yE_z \\ E_xE_z \\ E_xE_y \end{bmatrix}. \quad (4.16)$$

$$\frac{1}{\tilde{n}^2} = \begin{pmatrix} \frac{1}{n_x^2} + \Delta\left(\frac{1}{n^2}\right)_1 & \Delta\left(\frac{1}{n^2}\right)_6 & \Delta\left(\frac{1}{n^2}\right)_5 \\ \Delta\left(\frac{1}{n^2}\right)_6 & \frac{1}{n_y^2} + \Delta\left(\frac{1}{n^2}\right)_2 & \Delta\left(\frac{1}{n^2}\right)_4 \\ \Delta\left(\frac{1}{n^2}\right)_5 & \Delta\left(\frac{1}{n^2}\right)_4 & \frac{1}{n_z^2} + \Delta\left(\frac{1}{n^2}\right)_3 \end{pmatrix}. \quad (4.17)$$

Since the field-induced perturbations are symmetric, so the symmetry of the tensor is not disturbed. The presence of cross terms indicates that the ellipsoid is rotated and the lengths of the principal dielectric axes are changed. Mathematically, the electro-optic effect can be best represented as a deformation of the index ellipsoid because of an external electric field. The general form of the optical indicatrix if the axes do not necessarily correspond to the principal dielectric axes is

$$\frac{x^2}{\tilde{n}_1^2} + \frac{y^2}{\tilde{n}_2^2} + \frac{z^2}{\tilde{n}_3^2} + \frac{2yz}{\tilde{n}_4^2} + \frac{2xz}{\tilde{n}_5^2} + \frac{2xy}{\tilde{n}_6^2} = 1 \quad (4.18)$$

or equivalently,  $\mathbf{X}^T \frac{1}{\tilde{n}^2} \mathbf{X} = 1$  where  $\mathbf{X} = [x \ y \ z]$ . In other words,

$$\begin{aligned} \left[ \frac{1}{n_x^2} + \Delta\left(\frac{1}{n^2}\right)_1 \right] x^2 + \left[ \frac{1}{n_y^2} + \Delta\left(\frac{1}{n^2}\right)_2 \right] y^2 + \left[ \frac{1}{n_z^2} + \Delta\left(\frac{1}{n^2}\right)_3 \right] z^2 \\ + 2\Delta\left(\frac{1}{n^2}\right)_4 yz + 2\Delta\left(\frac{1}{n^2}\right)_5 xz + 2\Delta\left(\frac{1}{n^2}\right)_6 xy = 1. \end{aligned} \quad (4.19)$$

The index ellipsoid in the presence of an electric field can be written as

$$\begin{aligned} \left( \frac{1}{n_x^2} + r_{1k}E_k \right) x^2 + \left( \frac{1}{n_y^2} + r_{2k}E_k \right) y^2 + \left( \frac{1}{n_z^2} + r_{3k}E_k \right) z^2 \\ + 2yzr_{4k}E_k + 2xsr_{5k}E_k + 2xyr_{6k}E_k = 1 \end{aligned} \quad (4.20)$$

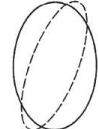
Here  $\Delta(1/n^2)_i = r_{ik}E_k$  with new index  $i = 1, 2, \dots, 6$  and  $k = x, y, z$ , and  $r_{ik}$  are the elements of the linear electro-optic tensor in contracted notation and  $E_x, E_y, E_z$  are the components of the applied electrical field in principal coordinates. A new set of principal axes  $x'$ ,  $y'$ , and  $z'$  can always be found by a coordinate rotation where the perturbed ellipsoid will be represented again in the standard form. Determining the new orientation and shape of the ellipsoid requires that  $1/\tilde{n}^2$  be diagonalized, thus determining its eigenvalues and eigenvectors. The perturbed ellipsoid will then be represented by a square sum:

$$\frac{x'^2}{n_{x'}^2} + \frac{y'^2}{n_{y'}^2} + \frac{z'^2}{n_{z'}^2} = 1. \quad (4.21)$$

Eigenvalues  $1/n_{x'}^2$ ,  $1/n_{y'}^2$ , and  $1/n_{z'}^2$ , depending on the strength and direction of the applied field and of course on the given matrix elements  $r_{ik}$  for the used crystal class.

The index ellipsoid is modified as a result of applying a steady electric field. How to find the new refractive indices or the modified principal refractive indices – to determine the optical properties of an anisotropic material exhibiting the Pockels effect?

1. Find the principal axes and the principal refractive indices  $n_1$ ,  $n_2$ , and  $n_3$  in the absence of the electric field or  $\mathbf{E} = 0$ .
2. Find the coefficients  $\{r_{ijk}\}$  from the crystal structure by using the appropriate matrix for  $r_{ik}$ .
3. Determine the impermeability tensor using:



$$\eta_{ij}(E) = \eta_{ij}(0) + \sum_k r_{ijk} E_k \quad (4.22)$$

where  $\eta_{ij}(0)$  is a diagonal matrix with elements  $1/n_x^2$ ,  $1/n_y^2$  and  $1/n_z^2$ .

4. Write the equation for the modified index ellipsoid:

$$\sum_{ij} \eta_{ij} x_i x_j = 1 \quad (4.23)$$

where  $\eta = 1/n^2$ .

5. Determine the principal axes of the new index ellipsoid by diagonalizing the matrix  $\eta_{ij}(E)$  and find the corresponding refractive indices  $n_1(E)$ ,  $n_2(E)$  and  $n_3(E)$ .
6. Given the direction of light propagation, find the normal modes and their associated refractive indices by using the index ellipsoid (Figure 4.3).

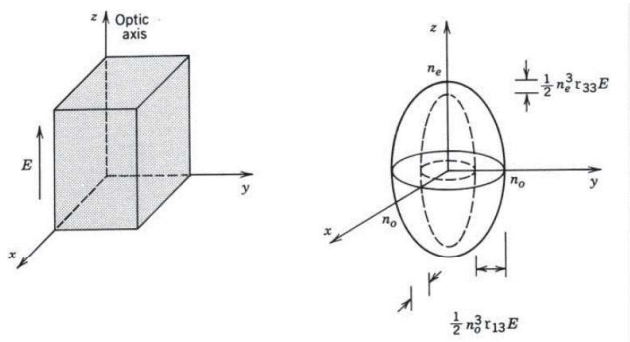


**Figure 4.3:** Modification of the index ellipsoid of a trigonal 3m crystal caused by an electric field in the direction of optic axis.

Diagonalizing the matrix  $\eta_{ij}(E)$  gives

$$\begin{aligned} \frac{1}{n_{x'}^2} &= \frac{1}{n_x^2} + r_x E \\ \frac{1}{n_{y'}^2} &= \frac{1}{n_y^2} + r_y E. \\ \frac{1}{n_{z'}^2} &= \frac{1}{n_z^2} + r_z E \end{aligned} \quad (4.24)$$

Since  $r_x E$ ,  $r_y E$  and  $r_z E$  terms are small – using  $(1 + a)^{-1/2} = 1 - \frac{1}{2} a$  for  $a \ll 1$ ,

$$\begin{aligned} n_{x'} &\approx n_x - \frac{1}{2} n_x^3 r_x E \\ n_{y'} &\approx n_y - \frac{1}{2} n_y^3 r_y E \\ n_{z'} &\approx n_z - \frac{1}{2} n_z^3 r_z E \end{aligned} \quad (4.25)$$

where  $n_x$  and  $n_y$  are the unperturbed indices of refraction and  $r_x$ ,  $r_y$  are the corresponding electro-optic coefficients for the used material and orientation of the applied field.

## The linear electro-optic coefficient matrices for crystal symmetry classes

The electro-optic tensor  $r_{ij}$  describes how the crystal responds to a field along any direction. The linear electro-optic coefficient matrices in contracted form for all crystal symmetry classes – keep in mind that the symbol over each matrix is the conventional symmetry-group designation:

### Triclinic:

$$\begin{matrix} 1^* \\ \left( \begin{array}{ccc} r_{11} & r_{12} & r_{13} \\ r_{21} & r_{22} & r_{23} \\ r_{31} & r_{32} & r_{33} \\ r_{41} & r_{42} & r_{43} \\ r_{51} & r_{52} & r_{53} \\ r_{61} & r_{62} & r_{63} \end{array} \right) \end{matrix}$$

### Cubic:

$$\begin{matrix} \bar{4}3m, 23 \\ \left( \begin{array}{ccc} 0 & 0 & 0 \\ 0 & 0 & 0 \\ 0 & 0 & 0 \\ r_{41} & 0 & 0 \\ 0 & r_{41} & 0 \\ 0 & 0 & r_{41} \end{array} \right) \end{matrix} \quad \begin{matrix} 432 \\ \left( \begin{array}{ccc} 0 & 0 & 0 \\ 0 & 0 & 0 \\ 0 & 0 & 0 \\ 0 & 0 & 0 \\ 0 & 0 & 0 \\ 0 & 0 & 0 \end{array} \right) \end{matrix}$$

### Orthorhombic:

$$\begin{matrix} 222 \\ \left( \begin{array}{ccc} 0 & 0 & 0 \\ 0 & 0 & 0 \\ 0 & 0 & 0 \\ r_{41} & 0 & 0 \\ 0 & r_{52} & 0 \\ 0 & 0 & r_{63} \end{array} \right) \end{matrix} \quad \begin{matrix} 2mm \\ \left( \begin{array}{ccc} 0 & 0 & r_{13} \\ 0 & 0 & r_{23} \\ 0 & 0 & r_{33} \\ 0 & r_{42} & 0 \\ r_{51} & 0 & 0 \\ 0 & 0 & 0 \end{array} \right) \end{matrix}$$

### Monoclinic:

$$\begin{matrix} 2 (2 \parallel x_2) \\ \left( \begin{array}{ccc} 0 & r_{12} & 0 \\ 0 & r_{22} & 0 \\ 0 & r_{32} & 0 \\ r_{41} & 0 & r_{43} \\ 0 & r_{52} & 0 \\ 6_{61} & 0 & r_{63} \end{array} \right) \end{matrix} \quad \begin{matrix} 2 (2 \parallel x_3) \\ \left( \begin{array}{ccc} 0 & 0 & r_{13} \\ 0 & 0 & r_{23} \\ 0 & 0 & r_{33} \\ r_{41} & r_{42} & 0 \\ r_{51} & r_{52} & 0 \\ 0 & 0 & r_{63} \end{array} \right) \end{matrix} \quad \begin{matrix} m (m \perp x_2) \\ \left( \begin{array}{ccc} r_{11} & 0 & r_{13} \\ r_{21} & 0 & r_{23} \\ r_{31} & 0 & r_{33} \\ 0 & r_{42} & 0 \\ r_{51} & 0 & r_{53} \\ 0 & r_{62} & 0 \end{array} \right) \end{matrix} \quad \begin{matrix} m (m \perp x_3) \\ \left( \begin{array}{ccc} r_{11} & r_{12} & 0 \\ r_{21} & r_{22} & 0 \\ r_{31} & r_{32} & 0 \\ 0 & 0 & r_{43} \\ 0 & 0 & r_{53} \\ r_{61} & r_{62} & 0 \end{array} \right) \end{matrix}$$

### Tetragonal:

$$\begin{matrix} 4 \\ \left( \begin{array}{ccc} 0 & 0 & r_{13} \\ 0 & 0 & r_{13} \\ 0 & 0 & r_{33} \\ r_{41} & r_{51} & 0 \\ r_{51} & -r_{41} & 0 \\ 0 & 0 & 0 \end{array} \right) \end{matrix} \quad \begin{matrix} \bar{4} \\ \left( \begin{array}{ccc} 0 & 0 & r_{13} \\ 0 & 0 & -r_{13} \\ 0 & 0 & 0 \\ r_{41} & -r_{51} & 0 \\ r_{51} & r_{41} & 0 \\ 0 & 0 & r_{63} \end{array} \right) \end{matrix} \quad \begin{matrix} 422 \\ \left( \begin{array}{ccc} 0 & 0 & 0 \\ 0 & 0 & 0 \\ 0 & 0 & 0 \\ r_{41} & 0 & 0 \\ 0 & -r_{41} & 0 \\ 0 & 0 & 0 \end{array} \right) \end{matrix} \quad \begin{matrix} 4mm \\ \left( \begin{array}{ccc} 0 & 0 & r_{13} \\ 0 & 0 & r_{13} \\ 0 & 0 & r_{33} \\ 0 & r_{51} & 0 \\ r_{51} & 0 & 0 \\ 0 & 0 & 0 \end{array} \right) \end{matrix} \quad \begin{matrix} \bar{4}2m (2 \parallel x_1) \\ \left( \begin{array}{ccc} 0 & 0 & 0 \\ 0 & 0 & 0 \\ 0 & 0 & 0 \\ r_{41} & 0 & 0 \\ 0 & r_{41} & 0 \\ 0 & 0 & r_{63} \end{array} \right) \end{matrix}$$

### Trigonal:

$$\begin{matrix} 3 \\ \left( \begin{array}{ccc} r_{11} & -r_{22} & r_{13} \\ -r_{11} & -r_{22} & r_{13} \\ 0 & 0 & r_{33} \\ r_{41} & r_{51} & 0 \\ r_{51} & -r_{41} & 0 \\ -r_{22} & -r_{11} & 0 \end{array} \right) \end{matrix} \quad \begin{matrix} 32 \\ \left( \begin{array}{ccc} r_{11} & 0 & 0 \\ -r_{11} & 0 & 0 \\ 0 & 0 & 0 \\ r_{41} & 0 & 0 \\ 0 & -r_{41} & 0 \\ 0 & -r_{11} & 0 \end{array} \right) \end{matrix} \quad \begin{matrix} 3m (m \perp x_1) \\ \left( \begin{array}{ccc} 0 & -r_{22} & r_{13} \\ 0 & r_{22} & r_{13} \\ 0 & 0 & r_{33} \\ 0 & r_{51} & 0 \\ r_{51} & 0 & 0 \\ -r_{22} & 0 & 0 \end{array} \right) \end{matrix} \quad \begin{matrix} 3m (m \perp x_2) \\ \left( \begin{array}{ccc} r_{11} & 0 & r_{13} \\ -r_{11} & 0 & r_{13} \\ 0 & 0 & r_{33} \\ 0 & r_{51} & 0 \\ r_{51} & 0 & 0 \\ 0 & -r_{11} & 0 \end{array} \right) \end{matrix}$$

**Hexagonal:**

$$\begin{pmatrix} 0 & 0 & r_{13} \\ 0 & 0 & r_{13} \\ 0 & 0 & r_{33} \\ r_{41} & r_{51} & 0 \\ r_{51} & -r_{41} & 0 \\ 0 & 0 & 0 \end{pmatrix} \begin{pmatrix} 0 & 0 & r_{13} \\ 0 & 0 & r_{13} \\ 0 & 0 & r_{33} \\ 0 & r_{51} & 0 \\ r_{51} & 0 & 0 \\ 0 & 0 & 0 \end{pmatrix} \begin{pmatrix} 0 & 0 & 0 \\ 0 & 0 & 0 \\ 0 & 0 & 0 \\ r_{41} & 0 & 0 \\ 0 & -r_{41} & 0 \\ 0 & 0 & 0 \end{pmatrix} \begin{pmatrix} r_{11} & -r_{22} & 0 \\ -r_{11} & r_{22} & 0 \\ 0 & 0 & 0 \\ 0 & 0 & 0 \\ 0 & 0 & 0 \\ -r_{22} & r_{11} & 0 \end{pmatrix} \begin{pmatrix} 0 & -r_{22} & 0 \\ 0 & r_{22} & 0 \\ 0 & 0 & 0 \\ 0 & 0 & 0 \\ 0 & 0 & 0 \\ -r_{22} & 0 & 0 \end{pmatrix} \begin{pmatrix} r_{11} & 0 & 0 \\ -r_{11} & 0 & 0 \\ 0 & 0 & 0 \\ 0 & 0 & 0 \\ 0 & 0 & 0 \\ 0 & -r_{11} & 0 \end{pmatrix}$$

**Centrosymmetric ( $\bar{1}$ , 2/m, mmm, 4/m, 4/mmm,  $\bar{3}$ ,  $\bar{3}m$ , 6/m, 6/mmm, m3, m3m):**

$$\begin{pmatrix} 0 & 0 & 0 \\ 0 & 0 & 0 \\ 0 & 0 & 0 \\ 0 & 0 & 0 \\ 0 & 0 & 0 \\ 0 & 0 & 0 \end{pmatrix}$$

## Modulator devices

An electro-optic modulator is a device with operation based on an electrically induced change in index of refraction or change in natural birefringence. Two types of modulators can be classified: longitudinal and transversal ones (Figure 4.4).

In the longitudinal configuration the voltage is applied parallel to the direction of light propagation in the device. The electrodes must be transparent for the light or a small aperture at the center at each end of the crystal has to be introduced. The applied electric field inside the crystal is  $E = V/L$ , where  $L$  is the length of the crystal. The induced phase shift is proportional to the voltage  $V$  but not to physical dimensions of the device.

In transverse configuration the voltage is applied perpendicular to the direction of light propagation. The electrodes do not obstruct the light as it passes through the crystal. The applied electric field is  $E = V/d$ ,

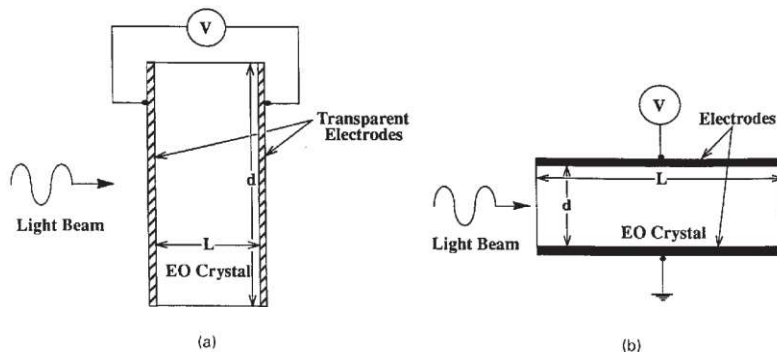


**Figure 4.4:** A longitudinal electro-optic modulator has the voltage applied parallel to the direction of light propagation (left); a transverse modulator has the voltage applied perpendicular to the direction of light propagation (right).

where  $d$  is the lateral separation of the electrodes. Thus, the voltage necessary to achieve a desired degree of modulation can be largely reduced by reduction of  $d$ . However, the transverse dimension  $d$  is limited by the increase of capacitance, which affects the modulation bandwidth or speed of the device.

## Modulation of Light Parameters

The modulation of polarization, phase, amplitude, frequency, and position of light can be implemented using an electro-optic bulk modulator with polarizers and passive birefringent elements. Usually it is desirable to modulate only one optical parameter at a time; simultaneous changes in the other parameters must then be avoided. Three assumptions are made:

1. First, it is assumed that the modulation field is uniform throughout the length of the crystal.
2. The modulation voltage is dc up to frequency

$$\omega_m \ll \frac{2\pi}{\tau} = \frac{2\pi c}{nL}. \quad (4.26)$$

The light experiences the same induced  $\Delta n$  during its transit time  $\tau$  through the crystal of length  $L$ , and the capacitance is negligible. Pockels cells typically can be operated at fairly low voltages (roughly 5 to 10 times less than an equivalent Kerr cell) and the response time is shorter than for Kerr cells. The response time of KDP is less than 10 ps, and such a modulator can work up to about 25 GHz. In LiNbO<sub>3</sub> electro-optic modulation up to 50 GHz has been demonstrated by Dolfi, D.W., Ranganath, T.R.: Electron. Lett. **28** (1992) 1197. High-speed modulators above 40 GHz for telecommunication applications in combination with semiconductor lasers today are mostly based on electro-absorption effect in some special semiconductor materials, see Takeuchi, H., Saito, T., Ito, H.: Technical Digest OFC2002, WV1. The following presentation corresponds widely to examples given in Yariv, A., Yeh, P.: Optical waves in crystals, New York: J. Wiley & Sons, 1984 and Maldonado, T.A.: Handbook of optics II, New York: McGraw-Hill, Inc., 1995, p. 13.1–13.35.

## Phase modulation

A light wave can be phase-modulated, without change in polarization or intensity, using a suitable cut of an electro-optic crystal. One of two possibilities is required for a crystal and its orientation:

1. A crystal having principal axes that will not rotate with applied voltage, but change refractive index uniformly. An example is LiNbO<sub>3</sub> with applied field along its optical z-axis. This solution is suitable for randomly polarized laser beams.
2. A crystal having a characteristic plane perpendicular to the direction of propagation where the plane rotates under the influence of an applied field. Then the input wave must be polarized along one of the new principal axes  $x'$  or  $y'$  and will not alter this polarization during modulation. An example is KDP with electric field applied along its optical z-axis. Such a configuration is shown in Figure 4.5.

For phase modulation, the input polarizer must be aligned parallel to one of the principal axes when the voltage is on or off. Figure 4.6 indicates a polarizer along  $x'$  with an input optical electric field

$$E_{i x'}^{\text{optical}}(t) = E_i^{\text{optical}} \cos(\omega_{\text{optical}} t) \quad (4.27)$$

the optical wave at the output of the crystal at  $z = L$  is

$$E_o^{\text{optical}} = E_i^{\text{optical}} \cos(\omega_{\text{optical}} t - \Gamma) \quad (4.28)$$

where

$$\Gamma = \frac{2\pi}{\lambda} (n_{x'} - \Delta n_{x'}) L = \Gamma_0 + \Gamma_i \quad (4.29)$$

is the total phase shift consisting of a natural phase term  $\Gamma_0 = (2\pi/\lambda)Ln_{x'}$ , with  $n_{x'}$  being the unperturbed index without applied electric field  $E$  in the  $x'$  direction, and an electrically-induced phase term

$$\Gamma_i = \Delta\Gamma = \frac{2\pi}{\lambda} \Delta n_{x'} L \quad (4.30)$$

for a polarization along  $x'$ , i.e. with a polarizer along  $x'$  the optical wave at the output of the crystal exhibits a phase shift. The electrically induced change in refractive index is  $\Delta n_{x'} \approx 1/2 n_{x'}^3 r E$ , where  $r$  is the corresponding electro-optic coefficient.

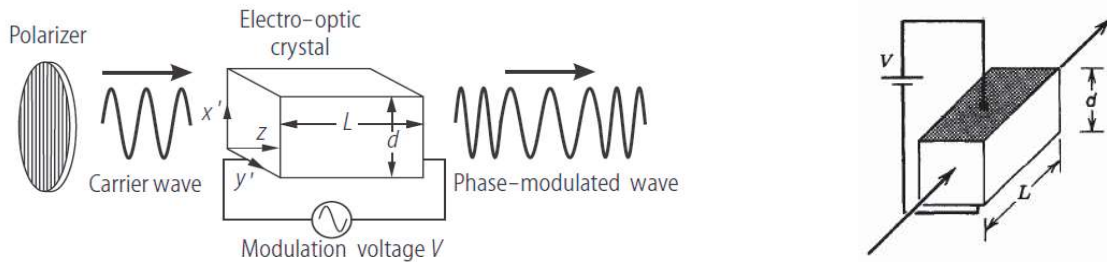


**Figure 4.5:** longitudinal phase modulator is shown with the light polarized along the new  $x'$  principal axis when the modulation voltage  $V$  is applied (left) and tangential (right) phase modulator.

For a longitudinal modulator with applied electrical field  $E = V/L$  the induced phase shift is (apart of sign)

$$\Delta\Gamma = \frac{\pi}{\lambda} n_{x'}^3 r V \quad (4.31)$$

which is independent of  $L$  and linearly proportional to  $V$ .

For a transverse modulator with applied electric field  $E = V/d$  the induced phase shift is

$$\Delta\Gamma = \frac{\pi}{\lambda} n_{x'}^3 r \left( \frac{L}{d} \right) V \quad (4.32)$$

which is a function of the aspect ratio  $L/d$ .

The half-wave voltage producing  $\Delta\varphi = \pi$  for a longitudinal modulator is

$$V_\pi = \frac{\lambda}{n_{x'}^3 r} \quad (4.33)$$

and for a transverse modulator

$$V_\pi = \frac{\lambda}{n_{x'}^3 r} \left( \frac{d}{L} \right). \quad (4.34)$$

Half-wave voltage is O(100 V) for transversal cells and O(1 kV) for longitudinal cells.

If a DC voltage is used, one of two possibilities is required for a crystal and its orientation. The first possibility is a crystal having principal axes which will not rotate with applied voltage  $V$ ; an example is LiNbO<sub>3</sub> with  $V$  applied in the  $z$  direction and an input polarization along the  $x' = x$  axis propagating along  $z' = z$ . The second possibility is a crystal having a characteristic plane perpendicular to the direction of propagation. If a field

is applied such that the axes rotate in this plane, the input wave must be polarized along one of the new principal axes. Therefore, it will always be polarized along a principal axis, whether the voltage is on or off. An example is KDP with  $V$  along the  $z$  axis and an input wave polarized along the new principal axis  $x'$  and propagating along  $z' = z$ . Phase modulation is then achieved by turning the voltage on and off.

If the applied modulation voltage is sinusoidal ( $V = V_m \sin \omega_m t$ ) and corresponding electric field is sinusoidal in time ( $E = E_m \sin \omega_m t$ ), i.e., the magnitude of the field varies only with time, not space; it is a stationary wave applied in the same direction for all time. In other words, this time-varying voltage signal is to be distinguished from a traveling wave voltage. In this case the phase at the output changes accordingly, as

$$\Gamma = \frac{2\pi}{\lambda} \Delta n L = \frac{2\pi}{\lambda} \left( n_{x'} - \frac{1}{2} n_{x'}^3 r E_m \sin \omega_m t \right) L = \Gamma_0 + \Gamma_m = \frac{2\pi}{\lambda} n_{x'} L - \delta \sin \omega_m t. \quad (4.35)$$

Thus, the optical field is phase-modulated with phase-modulation index

$$\delta = \frac{\pi}{\lambda} n_{x'}^3 r E_m L = \pi \frac{V_m}{V_\pi}. \quad (4.36)$$

Neglecting a constant phase term  $\Gamma_0$ , applying the identity

$$\cos(\delta \sin \omega_m t) + j \sin(\delta \sin \omega_m t) = e^{j\delta \sin \omega_m t} = \sum_{n=-\infty}^{\infty} J_n(\delta) e^{jn\omega_m t}. \quad (4.37)$$

By equating the real and imaginary parts the output wave can be developed into a Bessel function series

$$\begin{aligned} E_0^{\text{optical}}(t) &= E_i^{\text{optical}} \sum_n J_n(\delta) \cos(\omega_{\text{optical}} + n\omega_m)t \\ &= E_i^{\text{optical}} [J_0(\delta) \cos \omega t + J_1(\delta) \cos(\omega_{\text{optical}} + \omega_m)t - J_1(\delta) \cos(\omega_{\text{optical}} - \omega_m)t \\ &\quad + J_2(\delta) \cos(\omega_{\text{optical}} + 2\omega_m)t - J_2(\delta) \cos(\omega_{\text{optical}} - 2\omega_m)t] + \dots \end{aligned} \quad (4.38)$$

This consists of components at frequency  $\omega$  and higher harmonic frequencies ( $\omega_{\text{optical}} + n\omega_m$ ),  $n = \pm 1, \pm 2, \dots$  The distribution of energy into the sidebands is a function of modulation index  $\delta$ . For no modulation,  $\delta = 0$  and  $J_0(0) = 1$ ,  $J_1(0) = 0$  for  $n \neq 0$  and  $E_o = E_i \sin(\omega_{\text{optical}} t) = E_i x'(t)$ . For  $\delta \approx 2.4048$ ,  $J_0(\delta) = 0$  and all the power is transferred to harmonic frequencies.

## Polarization modulation (Dynamic Retardation)

Polarization modulation involves the coherent addition of two orthogonal waves, resulting in a change of the input polarization state at the output. A suitable configuration is shown in Figure 4.5. The crystal and applied voltage are configured to produce dynamically fast and slow axes in the crystal cross-section. The polarizer is positioned such that the input light is decomposed equally into the two orthogonal linear eigen-polarizations along these axes.

If the light propagating along the  $z$  principal axis is polarized along the  $x$ - (or  $y$ -) axis, the propagating fields are

$$\begin{aligned} E_{x'} &= E_0 \cos[\omega t - (2\pi/\lambda)n_{x'} z], \\ E_{y'} &= E_0 \cos[\omega t - (2\pi/\lambda)n_{y'} z], \end{aligned} \quad (4.40)$$

where the fast and slow axes are  $x'$  and  $y'$ . The corresponding refractive indices of the fast and slow axes  $x'$  and  $y'$ , respectively, are

$$\begin{aligned} n_{x'} &\approx n_x - \frac{1}{2} n_x^3 r_x E, \\ n_{y'} &\approx n_y - \frac{1}{2} n_y^3 r_y E, \end{aligned}$$

where  $n_x$  and  $n_y$  are the unperturbed indices of refraction in the absence of an applied field  $E$ , and  $r_x, r_y$  are the corresponding electro-optic coefficients for the used material and orientation of the applied field. As the two polarizations propagate at different speeds through the crystal, a phase difference (relative phase) or retardation  $\Gamma$  evolves between them as a function of length

$$\Gamma = \frac{2\pi}{\lambda} (n_{y'} - n_{x'})L = \frac{2\pi}{\lambda} (n_x - n_y)L + \frac{\pi}{\lambda} (n_x^3 r_x - n_y^3 r_y)EL = \Gamma_0 + \Gamma_i. \quad (4.38)$$

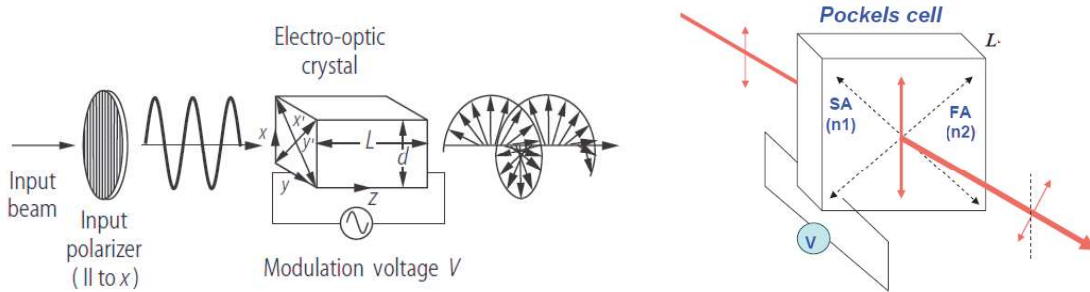


**Figure 4.5:** Longitudinal polarization modulator with input polarizer oriented along the  $x$  principal axis at 45 degrees with respect to the perturbed axes  $x'$  and  $y'$ .

$\Gamma_0$  is the natural retardation without applied field and  $\Gamma_i$  is the field-induced part of the retardation. In general, the output wave is elliptically polarized.

For a longitudinal modulator with applied electrical field  $E = V/L$  the induced phase shift is (apart of sign)

$$\Delta\Gamma = \Gamma_i = \frac{\pi}{\lambda} (n_x^3 r_x - n_y^3 r_y) V \quad (4.29)$$

which is independent of  $L$  and linearly proportional to  $V$ .

For a transverse modulator with applied electric field  $E = V/d$  the induced phase shift is

$$\Delta\Gamma = \Gamma_i = \frac{\pi}{\lambda} (n_x^3 r_x - n_y^3 r_y) \frac{L}{d} V \quad (4.30)$$

which is a function of the aspect ratio  $L/d$ .

The optical fields at the output can be expressed in terms of  $\Gamma$ :

$$\begin{aligned} E_{x'} &= \cos(\omega t) \\ E_{y'} &= \cos(\omega t - \Gamma) \end{aligned}$$

Therefore, the desired output polarization is obtained by applying the appropriate voltage magnitude. Figure 4.6 illustrates the evolution of the polarization state as a function of propagation distance  $z$ . In terms of an active device, Figure 4.6 can also be interpreted as a change in polarization state as a function of applied voltage for fixed length. The eigen-polarizations  $E_{x'}$  and  $E_{y'}$  are in phase at  $z = 0$ . They have the same frequency but different wavelengths. Light from one polarization gradually couples into the other. In the absence of natural birefringence,  $n_x - n_y = 0$ , the voltage that would produce a retardation  $\Gamma = \Gamma_i = 0$ , such that a vertical polarization input becomes a horizontal polarization output, is the half-wave voltage  $V_\pi$ .

For a longitudinal modulator

$$V_\pi = \frac{\lambda}{n_x^3 r_x - n_y^3 r_y} \quad (4.31)$$

which is independent of  $L$ , and for a transverse modulator

$$V_\pi = \frac{\lambda}{n_x^3 r_x - n_y^3 r_y} \left( \frac{d}{L} \right).$$

Special points are  $\Gamma = \pi/2$ , where the electrical field vector is circularly polarized, and  $\Gamma = \pi$ , where the wave is again linearly polarized, but rotated by  $90^\circ$  to its input direction of polarization. The half-wave voltage in this more general case of a longitudinal modulator is  $V_\pi = \lambda / (n_x^3 r_x - n_y^3 r_y)$ , which is proportional to the wavelength  $\lambda$  and inversely proportional to the relevant electro-optic coefficients. To cancel out an occurring natural birefringence, the phase retardation  $\Gamma_0$  can be made a multiple of  $2\pi$  by slightly polishing the crystal to adjust its length, or by introducing a variable compensator, or more practical by applying a bias voltage.

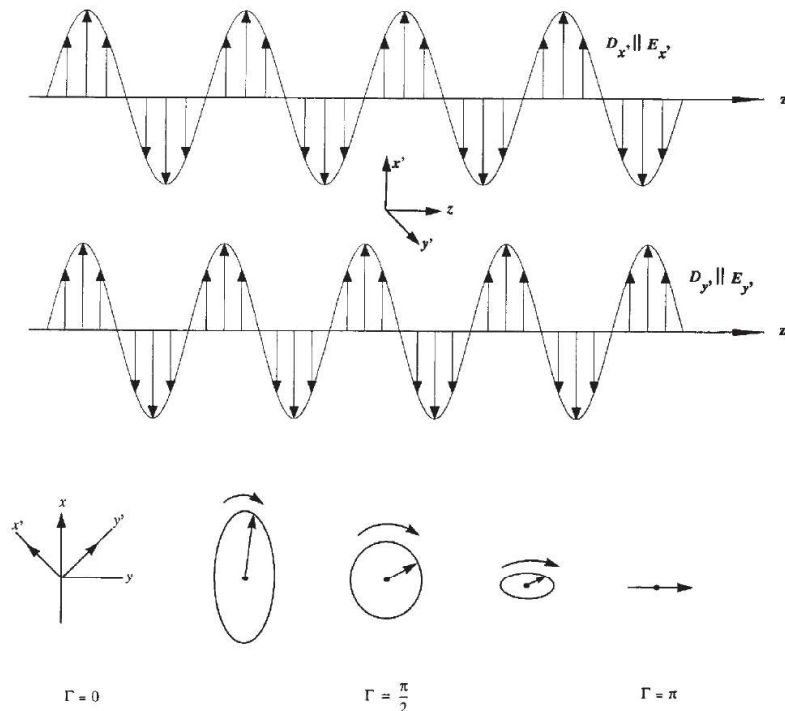


**Figure 4.6:** The polarization state of an input vertical linear polarization is shown as a function of crystal length  $L$  or applied voltage  $V$ . The retardation  $\Gamma = \pi$  for a given length  $L_\pi$  in a passive  $\lambda/2$  wave plate or applied voltage  $V_\pi$  in an electro-optic polarization modulator.

## Amplitude modulation

The intensity of a light wave can be modulated in several ways. Some possibilities are:

1. including a dynamic retarder configuration with either crossed or parallel polarizer at the output, or
2. using a phase modulator configuration in one branch of a Mach-Zehnder interferometer, or
3. choosing a dynamic retarder with push-pull electrodes.

An intensity modulator constructed using a dynamic retarder with crossed polarizers, as shown in Figure 4.6, yields for the transmission  $T = I_o/I_i$ , the ratio of output to input intensity,

$$T(V) = \sin^2\left(\frac{\Gamma}{2}\right) = \frac{1}{2} (1 - \cos \Gamma) = \frac{1}{2} \left[1 - \cos\left(\Gamma_0 + \frac{\pi V}{V_\pi}\right)\right]$$

For linear modulation around the 50% transmission point a fixed bias of  $\Gamma_0 = \pi/2$  must be introduced, either by placing an additional phase retarder, a quarter-wave plate at the crystal output, or by applying a bias voltage of  $V_\pi/2$ . In case of natural birefringence the values have to be changed accordingly.

For sinusoidal modulation of  $V$  the retardation at the output including bias is  $\Gamma = \pi/2 + \Gamma_m \sin \omega_m t$ , where the amplitude modulation index is

$$\Gamma_m = \pi \frac{V_m}{V_\pi}$$

The transmission in case of  $V_m \ll 1$  becomes

$$T(V) = \frac{1}{2}(1 + \Gamma_m \sin \omega_m t)$$

which is linear proportional to the modulation voltage. If the signal is large, then the output intensity becomes distorted, and again higher-order odd harmonics appear.

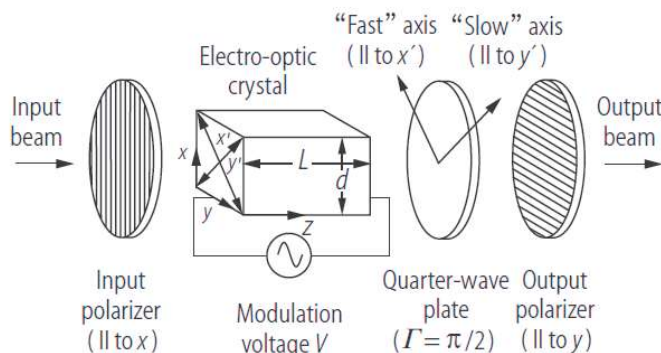


**Figure 4.5:** Longitudinal Intensity modulator using crossed polarizers and a quarter-wave plate as a bias to produce linear modulation.

## Design considerations

Modulators operating in transverse configuration have a half-wave voltage typically in the order of tens of volts compared to about 10,000 V for longitudinal devices. For phase modulation, a crystal orientation is required that would give the maximum change in index of refraction, whereas for amplitude modulation a maximum birefringence must be produced.

For  $L \ll 2\pi c / \omega_m n$  the transit time  $\tau = nL/c$  of light in the crystal is of no relevance for the modulation frequency and the electro-optic crystal can be modeled as a lumped capacitor. As the modulation frequency increases beyond such limit the optical phase no longer follows adiabatically the time-varying refractive index. The result is a reduction in the modulation index parameters,  $\delta$  for phase modulation and  $\Gamma_m$  for amplitude modulation, by a factor

$$\sigma = \frac{\sin\left(\frac{1}{2}\omega_m\tau\right)}{\frac{1}{2}\omega_m\tau} = \text{sinc}\left(\frac{1}{2}\omega_m\tau\right)$$

If  $\tau = 2\pi/\omega_m$  then the transit time of light is equal to the modulation period and the net retardation is reduced to zero. If, somewhat arbitrarily, one takes the highest useful modulation frequency from  $\tau = \pi/\omega_m$  it follows  $(v_m)_{\max} = c/(2Ln)$ . E.g. using a KDP crystal ( $n = 1.5$ ) with a length of  $L = 2$  cm, it yields  $(v_m)_{\max} = 5$  GHz.

## Traveling-wave modulator

Applying the modulation voltage as a traveling wave, propagating collinearly with the optical wave, can largely extend the limitation of the transit time on the bandwidth of a modulator. Figure 4.6 illustrates a transverse traveling-wave modulator. (The modulation field direction is along the x-axis, whereas both light and traveling wave propagate along z.) The electrode is designed to be part of the driving transmission line in order to eliminate electrode charging time effects on the bandwidth. Therefore, the transit time problem is addressed by adjusting the phase velocity of the modulation signal to be equal to the phase velocity of the optical signal.

A mismatch in the phase velocities of the modulating signal and optical wave will produce a reduction in the modulation index  $\delta$  or  $\Gamma_m$  by a factor

$$\sigma = \text{sinc}(qL)$$

where

$$q = \frac{\omega_m}{2c} (n_m - n) = \frac{\omega_m}{2} \left( \frac{1}{v_m} - \frac{1}{v_0} \right)$$

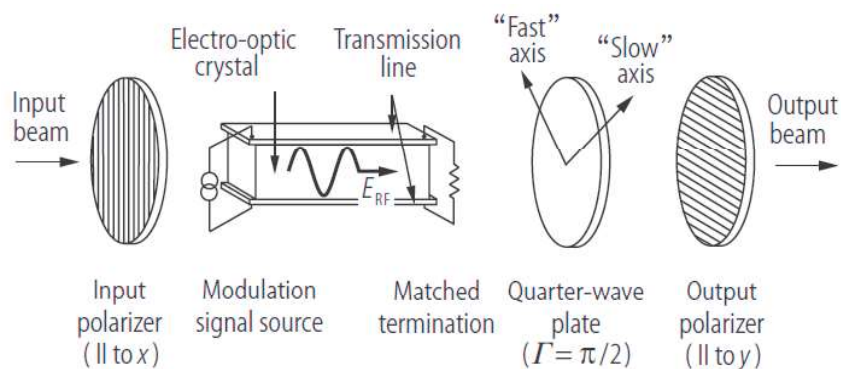


**Figure 4.6:** Transverse traveling-wave electro-optic modulator.

$v_m$  and  $n_m = \sqrt{\varepsilon}$  are the phase velocity and index of refraction of the modulating signal,  $v_0$  and  $n$  are the according terms for the light beam, respectively. In the case of amplitude modulation this equation holds only if there is no natural birefringence in the cross section of the crystal. Whereas for low frequencies the modulation indices  $\delta$  and  $\Gamma_m$  are linearly proportional to the crystal length  $L$  these become a sinusoidal function of  $L$  at higher frequencies. For a given mismatch  $q$  the maximum modulation index can be achieved for crystal lengths  $L = \pi/2q, 3\pi/2q$ , etc. The always occurring mismatch between  $n_m$  and  $n$  produces a walk-off between the optical wave and the modulation wave. The maximum useful modulation frequency is taken to be  $(v_m)_{\max} = c/[2L(n_m - n)]$ , showing an increase in the modulation frequency limit or useful crystal length by a factor of  $(1 - \frac{n_m}{n})^{-1}$  for a traveling-wave modulator.

# START HERE

## Materials exhibiting the Pockels Effect

A crystal can always be divided into a fundamental shape with a characteristic shape, volume, and contents. In many crystals, the unit cell may be chosen as a cube, with atoms placed at various points. All lattice planes and lattice directions are described by a mathematical description known as a Miller Index. This allows the specification, investigation, and discussion of specific planes and directions of a crystal. In the cubic lattice system, the direction  $(hkl)$  defines a vector direction normal to surface of a particular plane or facet, for instance, we refer to various directions in the crystal as  $(100)$ ,  $(110)$ , and  $(111)$ .as indicated in Figures 4.4 and 4.5.

Figure 4.6 shows the Miller Index for different lattice planes.

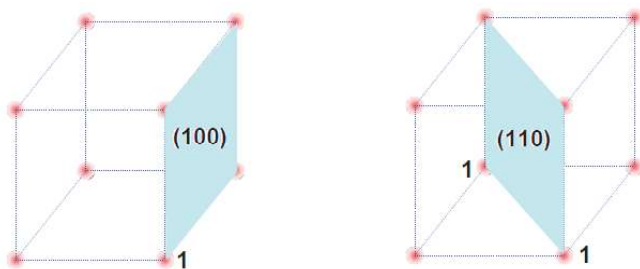


**Figure 4.4:** 100 and 110 plane in a crystal.

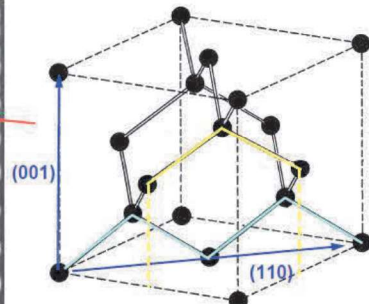
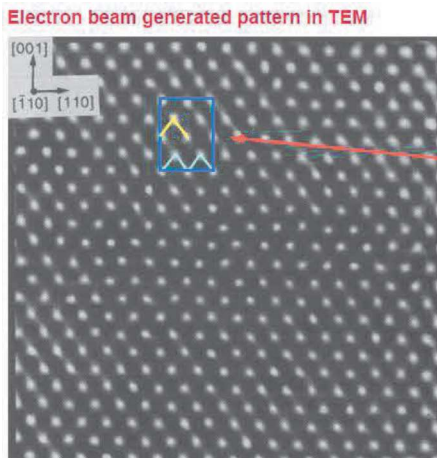


**Figure 4.5:** Crystal direction (110).

How are these directions determined?

We want the normal to the surface. As an example, consider a cube and a plane, in such a way that the plane has intercepts:  $x = a/2$ ,  $y = 2a/3$ ,  $z = a$ , or  $(1/2a, 2/3a, 1a)$ . Since we want normal to  $(1/2a, 2/3a, 1a)$ , inverting them  $(2a, 3/2a, a)$  gives the direction of the normal vector. Then taking the lowest common set of integers:  $(4,3,2)$  are the Miller indices of the plane (Figure 4.7).

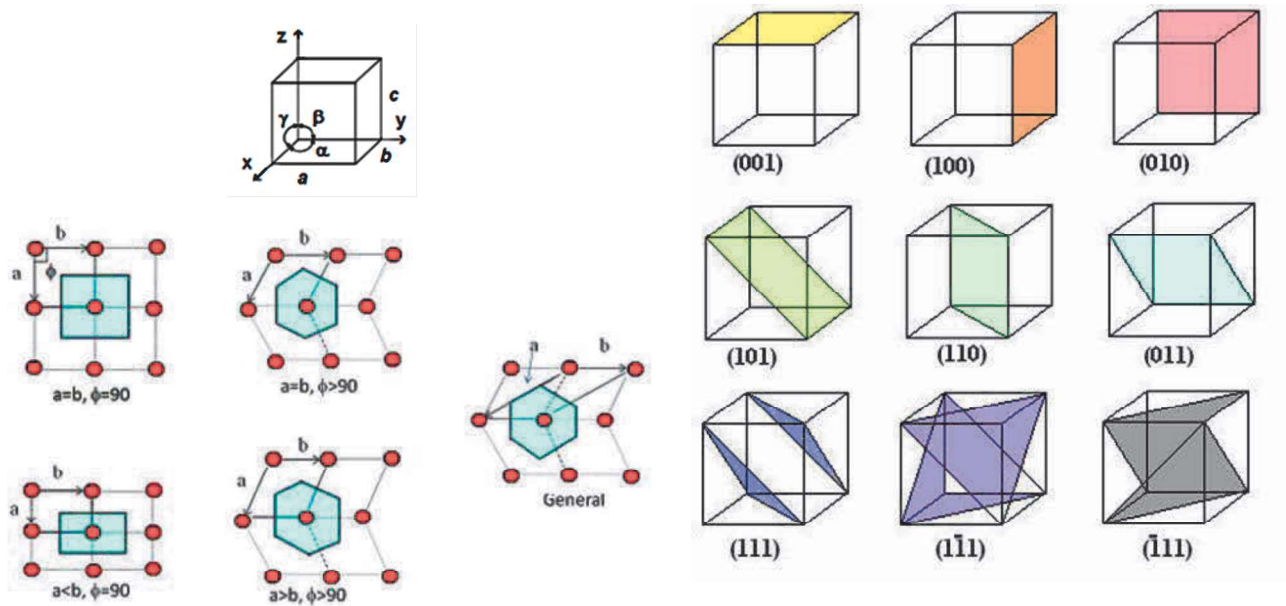


**Figure 4.6:** Crystal Planes.

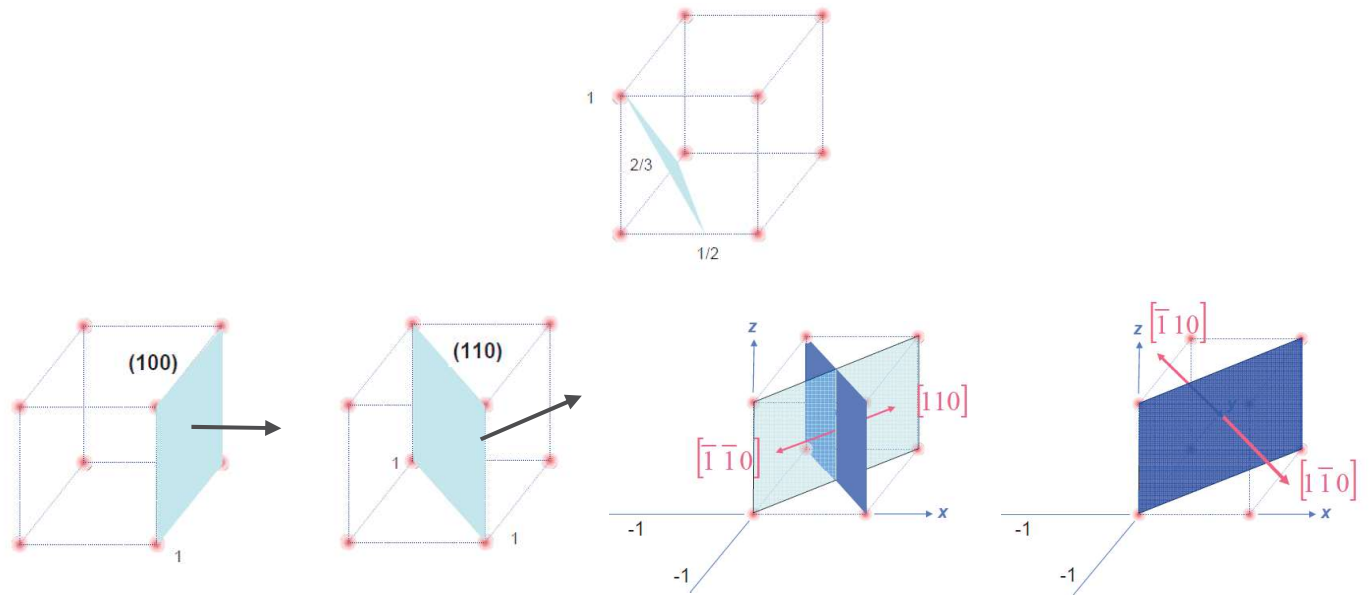


**Figure 4.7:** Plane  $(1/2a, 2/3a, 1a)$  shown in the top figure and normal to the  $(011)$  planes in bottom figures.

## LiTaO<sub>3</sub> (LTO) and LiNbO<sub>3</sub> Crystals

LiTaO<sub>3</sub> (LTO) or LiNbO<sub>3</sub> are trigonal (3m) crystals are uniaxial with  $n_x = n_y = n_o$ ,  $n_z = n_e$ , and the matrix  $r$ :

$$\begin{bmatrix} 0 & -r_{22} & r_{13} \\ 0 & r_{22} & r_{13} \\ 0 & 0 & r_{33} \\ 0 & r_{51} & r_{43} \\ r_{51} & 0 & 0 \\ -r_{22} & 0 & 0 \end{bmatrix}$$

Note that  $r_{113} = r_{13}$ ,  $r_{123} = r_{63} = 0$ ,  $r_{133} = r_{53} = 0$  and  $r_{223} = r_{23} = r_{13}$ ,  $r_{213} = r_{63} = 0$ ,  $r_{233} = r_{43} = 0$ , and  $r_{333} = r_{33} = r_{13}$ ,  $r_{313} = r_{53} = 0$ ,  $r_{323} = r_{43} = 0$ .

### z-cut or (100) cut – along (100) plane

An electric field is applied through the voltage  $V$  along the  $z$  axis, meaning that the electric field  $\mathbf{E} = (0, 0, E_z)$  points along the optic axis, therefore  $\eta_{ij}(E_z) = \eta_{ij}(0) + r_{ij3}E_z$  where  $\eta_{ij}(0)$  is a diagonal matrix with elements  $1/n_x^2$ ,  $1/n_y^2$  and  $1/n_z^2$ . Since  $\sum_{ij} \eta_{ij} x_i x_j = 1$  thus

$$\eta_{11}(E_z)x^2 + \eta_{22}(E_z)y^2 + \eta_{33}(E_z)z^2 = 1$$

since

$$\begin{cases} (\eta_{11}(0) + r_{13}E_z)x_1^2 = \left(\frac{1}{n_o^2} + r_{13}E_z\right)x^2 \\ (\eta_{22}(0) + r_{13}E_z)x_2^2 = \left(\frac{1}{n_o^2} + r_{13}E_z\right)y^2 \\ (\eta_{33}(0) + r_{33}E_z)x_3^2 = \left(\frac{1}{n_e^2} + r_{33}E_z\right)z^2 \end{cases}$$

the modified index ellipsoid is

$$\left(\frac{1}{n_o^2} + r_{13}E_z\right)(x^2 + y^2) + \left(\frac{1}{n_e^2} + r_{33}E_z\right)z^2 = 1$$

Determining the principal axes of the modified index ellipsoid by diagonalizing the matrix  $\eta_{ij}(\mathbf{E})$  and finding the corresponding refractive indices

$$\begin{cases} \frac{1}{n_o^2(E_z)} = \frac{1}{n_o^2} + r_{13}E_z \\ \frac{1}{n_e^2(E_z)} = \frac{1}{n_e^2} + r_{33}E_z. \end{cases}$$

Since  $r_{13}E$  and  $r_{33}E$  terms are small – using  $(1 + a)^{-1/2} = 1 - \frac{1}{2}a$  for  $a \ll 1$ ,

$$\begin{cases} n_x = n_y \approx n_o - \frac{1}{2}n_o^3 r_{13}E_z \\ n_z \approx n_e - \frac{1}{2}n_e^3 r_{33}E_z. \end{cases}$$

When an electric field is applied along the optic axis of this uniaxial crystal, it remains uniaxial with the same principal axes, but its refractive indices are modified (Figure 4.8).

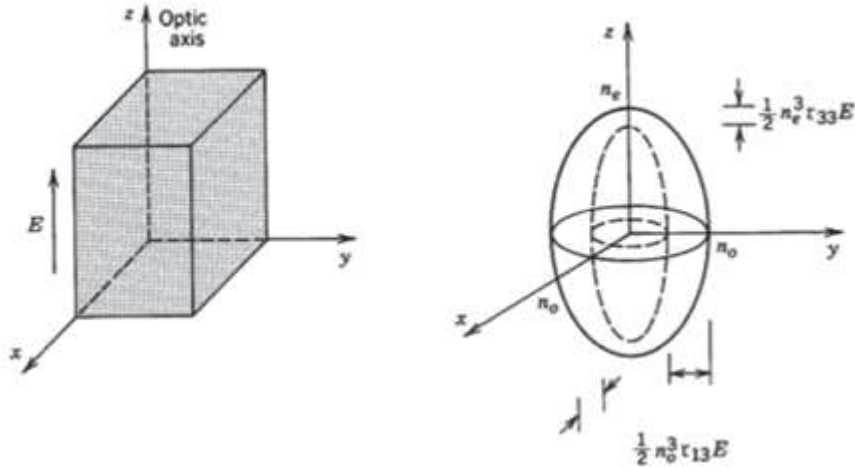


**Figure 4.8:** Modification of the index ellipsoid of a trigonal 3m crystal caused by an electric field in the direction of the optic axis.

#### x-cut or (011) cut – along (011) plane

For a x-cut (3m) transverse crystal LiTaO<sub>3</sub> (LTO) or LiNbO<sub>3</sub> with a beam along the x-axis and  $E$  along 45° between y and z

$$\Delta n = n_z - n_y = n_e - n_o - \frac{1}{2}(n_e^3 r_{33} - n_o^3 r_{13})E_x$$

$$\delta = \frac{2\pi(n_e - n_o)}{L} = \frac{2\pi\Delta n}{L}$$

#### GaAs, CdTe, and InAs Crystals

Cubic ( $\bar{4}3m$ ) crystals are isotropic ( $n_x = n_y = n_z = n$ ) with the matrix  $r$  (Figure ZE)

$$\begin{bmatrix} 0 & 0 & 0 \\ 0 & 0 & 0 \\ 0 & 0 & 0 \\ r_{41} & 0 & 0 \\ 0 & r_{41} & 0 \\ 0 & 0 & r_{41} \end{bmatrix}$$

An electric field is applied through the voltage  $V$  along the z axis, meaning that the electric field  $\mathbf{E} = (0, 0, E)$  points along the optic axis, the modified index ellipsoid is

$$\left( \frac{x^2 + y^2 + z^2}{n^2} \right) + 2r_{41}Exy = 1$$

The modified principal axes are obtained by rotating the coordinate system 45° about the z axis. Substituting  $x' = (x - y)/\sqrt{2}$ ,  $y' = (x + y)/\sqrt{2}$ ,  $z' = z$ ,

$$\frac{x'^2}{n_1^2(E)} + \frac{y'^2}{n_2^2(E)} + \frac{z'^2}{n_3^2(E)} = 1$$

where

$$\frac{1}{n_1^2(E)} = \frac{1}{n^2} + r_{41}E,$$

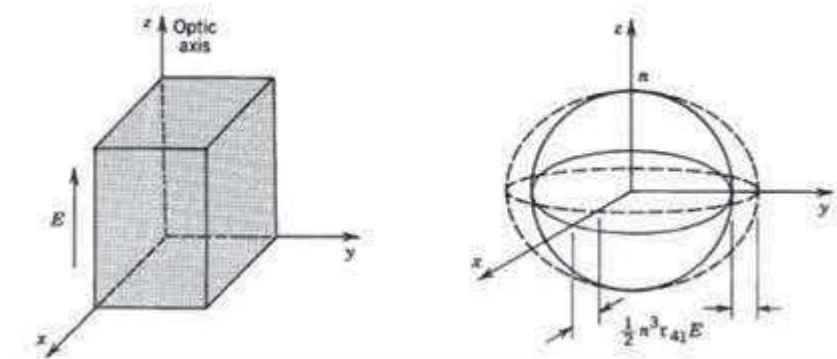


**Figure ZE:** Modification of the index ellipsoid of a trigonal  $\bar{4}3m$  crystal caused by an electric field in the direction of the optic axis.

$$\begin{aligned}\frac{1}{n_2^2(E)} &= \frac{1}{n^2} - r_{41}E, \\ n_3(E) &= n\end{aligned}$$

Therefore

$$\begin{aligned}n_1 &\approx n - \frac{1}{2} n_o^3 r_{41} E, \\ n_2 &\approx n - \frac{1}{2} n_e^3 r_{41} E, \\ n_3 &= n\end{aligned}$$

For a normal GaAs (100) crystal

$$\Delta n = n_{x'} - n_{y'} = n^3 r_{41} E_z$$

For a tangential GaAs (110) crystal

$$\Delta n = n_{x'} - n_{y'} = \frac{1}{2} n^3 r_{41} E_x$$

## KDP and ADP Crystals

For ( $\bar{4}2m$ ) crystals – like KDP and ADP – similar to uniaxial crystals with  $n_x = n_y = n_o$ ,  $n_z = n_e$ , and the matrix  $r$  (Figure ZF)

$$\begin{bmatrix} 0 & 0 & 0 \\ 0 & 0 & 0 \\ 0 & 0 & 0 \\ r_{41} & 0 & 0 \\ 0 & r_{41} & 0 \\ 0 & 0 & r_{63} \end{bmatrix}$$

An electric field is applied through the voltage  $V$  along the  $z$  axis, meaning that the electric field  $E = (0, 0, E)$  points along the optic axis, the modified index ellipsoid is

$$\left(\frac{x^2 + y^2}{n_o^2}\right) + \frac{z^2}{n_e^2} + 2r_{63}Exy = 1$$

The modified principal axes are obtained by rotating the coordinate system  $45^\circ$  about the  $z$  axis. Substituting  $x' = (x - y)/\sqrt{2}$ ,  $y' = (x + y)/\sqrt{2}$ ,  $z' = z$ ,

$$\frac{x'^2}{n_1^2(E)} + \frac{y'^2}{n_2^2(E)} + \frac{z'^2}{n_3^2(E)} = 1$$

where

$$\begin{aligned} \frac{1}{n_1^2(E)} &= \frac{1}{n_o^2} + r_{63}E, \\ \frac{1}{n_2^2(E)} &= \frac{1}{n_o^2} - r_{63}E, \\ n_3(E) &= n_e \end{aligned}$$

Therefore

$$\begin{aligned} n_1 &\approx n - \frac{1}{2}n_o^3r_{63}E, \\ n_2 &\approx n - \frac{1}{2}n_o^3r_{63}E, \\ n_3 &= n_e \end{aligned}$$

For a transverse E-field (normal incident)  $E = E_o(1-r)$  where

$$r = \left| \frac{n_t - n_r}{n_t + n_r} \right|$$

**Table A** presents the refractive index and EO coefficients for different EO materials.

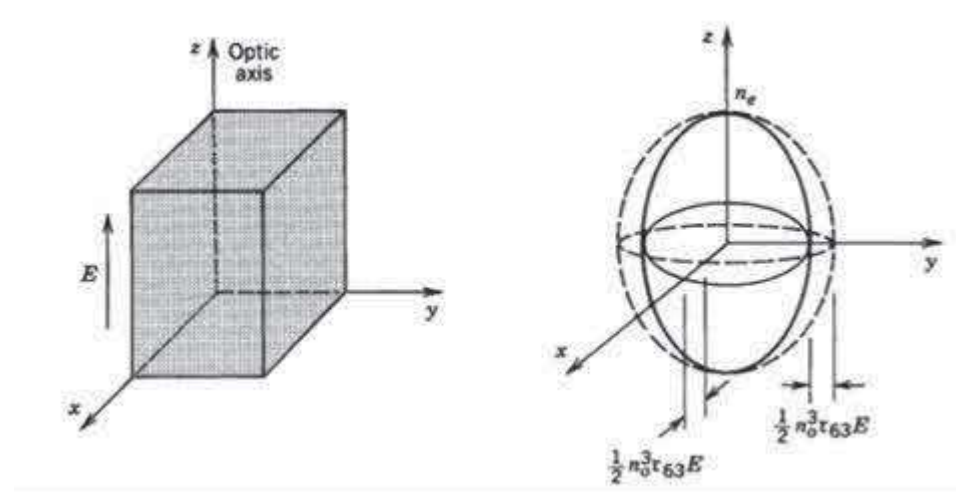


**Figure ZF:** Modification of the index ellipsoid of a trigonal  $\bar{4}2m$  crystal caused by an electric field in the direction of the optic axis.

**Table A:** Refractive Index and EO coefficients for different EO materials.

Material	Refractive Index (Optical)		EO coefficients (pm/V)		Electro-optic figure of merit ( $n^3r$ ) (pm/V)		Weighted figure of merit (pm/V)	
	$n_e$	$n_o$	$r_{33}$	$r_{13}$	T	N	T	N
LiNbO <sub>3</sub>	2.15	2.23	30.8	8.6	105.4	NA	<b>34</b>	<b>NA</b>
LiTaO <sub>3</sub>	2.18	2.176	33	7.5	132.3	NA	<b>35</b>	<b>NA</b>
ZnTe		2.85	4.3		49.8	99.5	<b>24</b>	<b>48</b>
CdTe		2.84	4.5		51.5	103.1	<b>25</b>	<b>51</b>
BSO		2.54	5		41.0	81.9	<b>10</b>	<b>20</b>
GaAs		3.43	1.43		28.9	57.7	<b>12</b>	<b>25</b>
ZnSe		2.6	2		17.6	35.2	<b>9</b>	<b>17</b>